Phycologia Volume 54 (2), 210–232 Published 14 April 2015

Cyst–theca relationship and phylogenetic positions of the diplopsalioideans (Peridiniales, Dinophyceae), with description of *Niea* and *Qia gen. nov.*

TINGTING LIU[1], KENNETH NEIL MERTENS[2] AND HAIFENG GU[1]*

[1]*Third Institute of Oceanography, SOA, Xiamen 361005, China*
[2]*Research Unit Palaeontology, Ghent University, Krijgslaan 281 S8, 9000 Gent, Belgium*

ABSTRACT: Nine genera have been assigned to the subfamily Diplopsalioideae, but since most have not been characterized molecularly and their cyst–theca relationships are largely unknown, the phylogenetic relationships among these genera are not well understood. Here we established the cyst–theca relationships of 11 species (*Boreadinium breve*, *Diplopelta globula*, *Diplopsalis lenticula*, *Diplopsalopsis ovata*, *Lebouraia pusilla*, *Niea acanthocysta*, *Niea chinensis*, *Niea torta*, *Oblea rotunda*, *Preperidinium* cf. *meunieri* and *Qia lebouriae*) belonging to nine genera by incubating cysts collected along the coast of China. In addition, we obtained 22 large-subunit ribosomal DNA sequences from the germinated motile cells of these 11 species by single-cell polymerase chain reaction. A new genus, *Niea*, was erected to encompass species with a plate formula identical to that of *Oblea*, that is, Po, X, 3′, 1a, 6″, 3C+t, 5‴, 2⁗, but with an ortho 1′. *Niea chinensis* was described based on both theca and cyst morphology. The genus *Oblea* was emended to incorporate only species with a meta 1′. As a consequence, *Oblea acanthocysta* and *O. torta* were transferred to the newly erected genus *Niea*. A second new genus, *Qia*, was established to encompass *Diplopsalis lebouriae*, and the genus *Diplopsalis* was emended, differing from *Qia* in the shape of the anterior intercalary (1a) plate. Phylogenetic analyses were carried out using maximum likelihood and Bayesian inference. Molecular phylogeny revealed that the diplopsalioideans were not monophyletic and were subdivided into three clades. From our results, the shape of the first apical and anterior intercalary plates and the number of apical, anterior intercalary and antapical plates were useful characteristics to distinguish the diplopsalioideans at the genus level.

KEY WORDS: *Boreadinium breve*, Cyst, *Diplopelta globula*, *Diplopsalis lenticula*, *Diplopsalopsis ovata*, *Lebouraia pusilla*, *Oblea acanthocysta*, *Oblea rotunda*, *Oblea torta*, *Qia lebouriae*

INTRODUCTION

The dinoflagellate subfamily Diplopsalioideae was included in the family Congruentidiaceae of the order Peridiniales together with another subfamily Congruentidioideae, characterized by four or five climactal plates, one antapical (fundital) plate or either of these features (Matsuoka 1988; Elbrächter 1993; Fensome *et al.* 1993). Species of Diplopsalioideae are predominantly marine (Abé 1941, 1981; Nie 1943; Dodge & Hermes 1981; Matsuoka 1988; Dodge & Toriumi 1993), but some species can also inhabit brackish water [e.g. *Oblea rotunda* (Lebour) Balech *ex* Sournia] (Chomérat *et al.* 2004) and freshwater [e.g. *Kolkwitziella acuta* (Apstein) Elbrächter] (Elbrächter 1993).

The genus *Diplopsalis* Bergh was characterized by a distinct left sulcal list with *Diplopsalis lenticula* Bergh as the type species (Bergh & Daday 1881). Like other armoured dinoflagellates, one plate difference in the epithecal or hypothecal series is sufficient to warrant placement in a different genus, and therefore several more genera (e.g. *Diplopelta* Stein, *Diplopsalopsis* Meunier, *Preperidinium* Mangin) were established subsequently based on the differences in the plate formulae (e.g. Pavillard 1913; Lebour 1922; Abé 1941, 1981; Taylor 1976; Dodge & Hermes 1981; Dodge & Toriumi 1993). Currently, 11 extant motile based genera were validly described (e.g. *Boreadinium* J.D. Dodge & H.B. Hermes, *Gotoius* T.H. Abé *ex* Matsuoka, *Oblea* Balech *ex* Loeblich Jr. & Loeblich III; see supplementary data Table S1), and these have been classified within the subfamily Diplopsalioideae.

The diplopsalioideans can be subdivided into two groups: a group with one antapical plate (*Boreadinium*, *Diplopsalis*, *Lebouraia* T. H. Abé *ex* Sournia and *Preperidinium*) and another group with two antapical plates (*Diplopelta*, *Diplopsalopsis*, *Gotoius*, *Oblea*; Abé 1941; Balech 1964; Dodge & Hermes 1981; Matsuoka 1988). Other morphological characteristics at the genus level include the number of apical, anterior intercalary and precingular plates (Dodge & Hermes 1981). Abé (1981, p. 20, fig. 2) put more emphasis on the taxonomic significance of the sulcal area in the diplopsalioideans and recognized two major types: one type with a small posterior sulcal (Sp) plate that he called the 'Caspica-type' and another type with a large Sp that he called the 'Asymmetrica-type'. Independently, Dodge and Hermes (1981) recognized three different arrangements of the anterior sulcal (Sa) plate and right sulcal (Sd) plate, which they called A-type, B-type and C-type.

Phylogenetic relationships among these genera in the diplopsalioideans still remain unverified because evidence from molecular phylogenies is limited (Gribble & Anderson 2006; Kawami *et al.* 2006). The available data suggest that some of these genera are polyphyletic (e.g. *Diplopsalis*; Matsuoka & Kawami 2013; Mertens *et al.* 2015).

Many diplopsalioideans species produce cysts that are generally brown and smooth (Matsuoka 1988; Lewis 1990). The only exceptions are *Oblea acanthocysta* Kawami, Iwataki

* Corresponding author (guhaifeng@tio.org.cn).
DOI: 10.2216/14-94.1

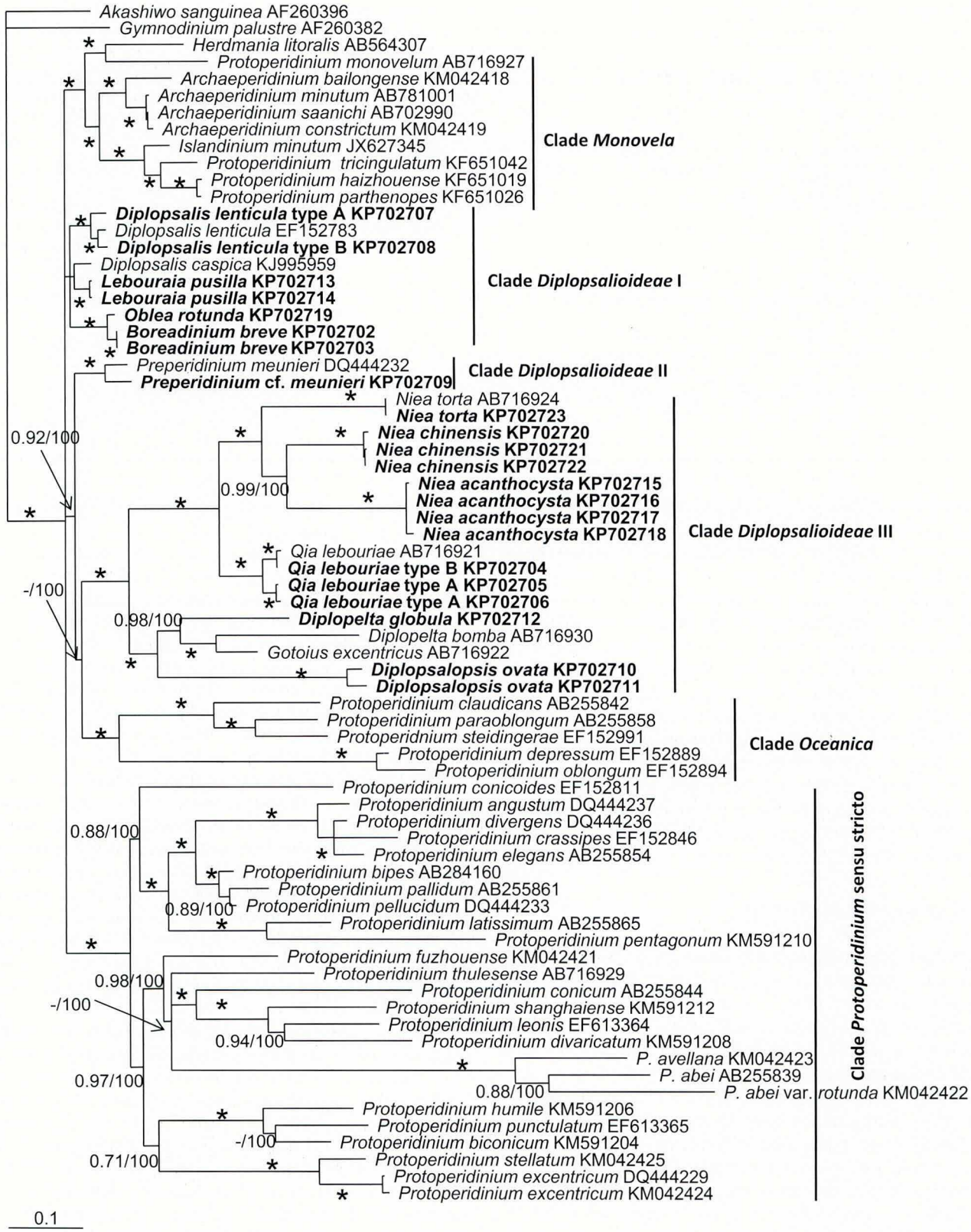

Fig. 1. A phylogenetic tree of the diplopsalioideans inferred from partial LSU rDNA sequences using Bayesian inference. *Akashiwo sanguinea* was selected as the out-group. Branch lengths are drawn to scale, with the scale bar indicating the number of the substitutions per site. Numbers on branches are statistical support values to clusters on the right of them (Bayesian posterior probability/MLbootstrap support). * indicates maximal support (Bayesian posterior probability: 1.00/ML bootstrap support: 100). Clades are labelled and marked with vertical lines on the right. New sequences obtained in this study are indicated in bold font.

Table 1. Station name, latitude (°N), longitude (°E), location name, collection date, water depth (m) and species encountered.

Station name	Latitude (°N)	Longitude (°E)	Location name	Collection date	Water depth (m)	Species encountered
Y1	39°14′59.49″	122°36′05.36″	Dalian (Yellow Sea)	25 Apr. 2011	20	*Boreadinium breve*, *Diplopsalis lenticula*, *Lebouraia pusilla*, *Niea acanthocysta*, *Niea chinensis*, *Qia lebouriae* type B
B1	38°56′59.95″	117°55′08.15″	Tianjin (Bohai Sea)	6 May 2011	15	*Oblea rotunda*
Y2	36°02′31.26″	120°17′02.04″	Qingdao (Yellow Sea)	8 May 2011	10	*D. lenticula*, *L. pusilla*, *N. acanthocysta*, *N. chinensis*, *Niea torta*
Y3	34°47′49.05″	119°31′07.99″	Lianyungang (Yellow Sea)	9 May 2011	12	*B. breve*, *Diplops. lenticula*, *Diplopsalopsis ovata*, *L. pusilla*, *N. chinensis*, *N. acanthocysta*, *N. torta*, *O. rotunda*, *Q. lebouriae* type A, *Q. lebouriae* type B, *Preperidinium* cf. *meunieri*
E1	30°35′59.00″	122°08′33.63″	Shanghai (East China Sea)	11 May 2011	20	*N. chinensis*, *O. rotunda*
E2	26°38′09.41″	19°47′13.17″	Ningde (East China Sea)	7 Jul. 2010	10	*D. lenticula*, *O. rotunda*
E3	24°49′25.26″	118°47′40.95″	Quanzhou (East China Sea)	7 Jun. 2010	12	*N. chinensis*, *O. rotunda*
S1	21°29′58.20″	108°13′53.20″	Fangchenggang (South China Sea)	28 Apr. 2011	15	*Diplopelta globula*, *Diplops. lenticula*, *Diplopsalo. ovata*, *L. pusilla*, *N. acanthocysta*, *N. chinensis*, *Q. lebouriae* type A, *Q. lebouriae* type B

& Matsuoka and *Diplopelta symmetrica* Pavillard, of which the former has a spiny and the latter a hairy cyst (Dale *et al.* 1993; Kawami *et al.* 2006). In contrast to cysts of *Protoperidinium* Bergh species, which often have a saphopylic archeopyle corresponding to 2a plate (Harland 1982), the diplopsalioideans always have a theropylic archeopyle, corresponding to suturing along predetermined plate boundaries (Matsuoka 1988; Lewis 1990; Dale *et al.* 1993). Wall and Dale (1968) first established cyst–theca relationships, and this has been followed by many other later studies (noted in supplementary data Table S1); however, the systematic importance of the cyst morphology has not been fully explored.

The purpose of the present study is to clarify the phylogenetic positions of the diplopsalioideans to confirm the validity of morphological characteristics that distinguish diplopsalioideans at the generic level.

MATERIAL AND METHODS

Surface sediment samples were collected along the coast of China with a small boat using a Van Veen grab between June 2010 and May 2011 (supplementary data Fig. S1; the precise locations are given in Table 1). All samples were stored in the dark at 4°C until further treatment. Approximately 5 g wet weight of sediment material were diluted in a 20-ml beaker with filtered seawater with a salinity of 30 and sonicated for 1 min in an ultrasonic bath (JY96 Xinzhi, Ningbo, China). The water slurry was rinsed with filtered seawater whilst sieving through a 20-μm nylon mesh. The fraction retained by the sieve was resuspended with 1 ml of filtered seawater and used for cyst isolation. Using a microscope BX51 (Olympus Corp., Tokyo, Japan), cysts were isolated with a micropipette into 96-well plates, with each well containing 300 μl of f/2-Si medium (Guillard & Ryther 1962). The plates were incubated at 20°C, 90 μmol photons m^{-2} s^{-1} with a 12:12 light:dark cycle and examined daily with an inverted microscope AE31 (Motic, Xiamen, China). A total of 83 cysts were germinated which generally yielded motile cells after 1–7 d of incubation.

After germination, both cell and cyst were individually transferred onto cleaned glass slides and examined at ×400 magnification with an Olympus BX51 light microscope with a digital camera (Qimaging, Burnaby, BC, Canada). No mounting medium was used. Calcofluor white was used to discern plates in vegetative cells (Fritz & Triemer 1985). For observation by scanning electron microscopy (SEM), the cell or cyst was fixed with buffered glutaraldehyde at a final concentration of 2.5% v/v for 1 h. They were transferred to a coverslip coated with poly-L-lysine (molecular weight 70,000–150,000) for 30 min and then washed for 10 min in a 1:1 solution of distilled water and filtered seawater, followed by a second wash in distilled water for 10 min. The samples were then dehydrated and critical point dried according to the method of Liu *et al.* (2014) and examined using a LEO 1530 Gemini SEM (Zeiss/LEO, Oberkochen, Germany). The Kofoidian system was used for designating the thecal plates (Fensome *et al.* 1993). All cyst and motile cell measurements in the species descriptions cite the minimum, average (in parentheses) and maximum values, in that order.

Identified cells were rinsed several times in sterilized distilled water, broken by squeezing the coverslip above and then transferred into a polymerase chain reaction (PCR) tube. Twenty-one germinated cells were used as the template to amplify about 1430 base pairs (bp) of the large-subunit ribosomal DNA (LSU rRNA gene; D1–D6 domains), using the primers D1R (forward, 5′-ACCCGCTGAATTTAAG CATA-3′; Scholin *et al.* 1994) and 28-1483R (reverse, 5′-GCTACTACCACCAAGATCTGC-3′; Daugbjerg *et al.* 2000). Approximately 650 bp of the LSU rDNA (D1–D2 domains) were obtained from one cell of *D. lenticula* (type A; see "Results") using the primers D1R and D2C (reverse, 5′-CCTTGGTCCCGTGTTTCAAGA-3′; Scholin *et al.* 1994). A 50-μl PCR cocktail containing 0.2 μM forward and reverse primer, PCR buffer, 50 μM dNTP and 1 U of Taq DNA

Table 2. Morphological characteristics of species examined in the present study and their LSU rDNA sequence information.

	Plate formula	1′	Anterior intercalary plates	Cyst	*	**
Boreadinium breve	Po, X, 4′, 1a, 6″, 3C+t, ?3S, 5‴, 1⁗	meta-type	1a large, touches plates 1″–5″	smooth	5, 2	KP702702, KP702703 (Lianyungang)
Diplopelta globula	Po, 3′, 2a, 6″, 3C+t, ?3S, 5‴, 2⁗	ortho-type	2a larger than 1a	smooth	1, 1	KP702712 (Fangchenggang)
Diplopsalis lenticula type A	Po, X, 3′, 1a, 6″, 3C+t, ?4S, 5‴, 1⁗	ortho-type	1a rectangular, in the lower part of the dorsal epitheca	smooth	8, 1	KP702707 (Dalian)
D. lenticula type B	Po, X, 3′, 1a, 6″, 3C+t, ?4S, 5‴, 1⁗	ortho-type	1a rectangular, in the lower part of the dorsal epitheca	smooth	2, 1	KP702708 (Fangchenggang)
Diplopsalopsis ovata	Po, X, 3′, 2a, 7″, 3C+t, ?3S, 5‴, 2⁗	ortho-type	2a larger than 1a	smooth	11, 2	KP702710, KP702711 (Fangchenggang)
Lebouraia pusilla	Po, X, 3′, 2a, 6″, 3C+t, ?3S, 5‴, 1⁗	meta-type	1a larger than 2a	smooth	11, 2	KP702713, KP702714 (Fangchenggang)
Niea acanthocysta	Po, X, 3′, 1a, 6″, 3C+t, ?4S, 5‴, 2⁗	ortho-type	1a hexagonal, in the middle of the dorsal epitheca	spiny	7, 3	KP702715–KP702718 (Fangchenggang)
N. chinensis	Po, X, 3′, 1a, 6″, 3C+t, ?4S, 5‴, 2⁗	ortho-type	1a hexagonal, in the middle of the dorsal epitheca	smooth	20, 3	KP702720–KP702722 (Fangchenggang)
N. torta	Po, X, 3′, 1a, 6″, 3C+t, ?4S, 5‴, 2⁗	ortho-type	1a hexagonal, inclined to the left of the dorsal epitheca	smooth	2, 1	KP702723 (Qingdao)
Oblea rotunda	Po, X, 3′, 1a, 6″, 3C+t, ?4S, 5‴, 2⁗	meta-type	1a large, touches plates 1″–5″	smooth	6, 1	KP702719 (Ningde)
Preperidinium cf. *meunieri*	Po, X, 3′, 2a, 7″, 3C+t, ?3S, 5‴, 2⁗	ortho-type	1a very small	smooth	1, 1	KP702709 (Lianyungang)
Qia lebouriae type A	Po, X, 3′, 1a, 6″, 3C+t, ?4S, 5‴, 1⁗	ortho-type	1a hexagonal, in the middle of the dorsal epitheca	hairy	3, 2	KP702705, KP702706 (Fangchenggang)
Q. lebouriae type B	Po, X, 3′, 1a, 6″, 3C+t, ?4S, 5‴, 1⁗	ortho-type	1a hexagonal, in the middle of the dorsal epitheca	spiny	7, 1	KP702704 (Fangchenggang)

* The number of cysts that germinated, the number of germinated cells used for sequencing.
** The accession numbers (origin of site from where the cyst was derived).

polymerase (Takara, Dalian, China) was subjected to 35 cycles using a Mastercycler PCR (Eppendorf, Hamburg, Germany). The PCR protocol was identical to that of Liu *et al.* (2015) and Gu *et al.* (2015). Sequences were deposited in GenBank with accession numbers KP702702–KP702723.

Sequences newly obtained were first aligned with those of related species available in GenBank using BioEdit v7.0.0 (Hall 1999) and then using Mafft (Katoh *et al.* 2005) (http://mafft.cbrc.jp/alignment/server/). *Akashiwo sanguinea* (Hirasaka) G. Hansen & Moestrup was selected as the out-group. The optimal model was chosen using jModelTest (Posada 2008). A general time reversible model (GTR+I+G) was selected with the Akaike information criterion. Maximum likelihood–based analyses were conducted with RAxML v7.2.6 (Stamatakis 2006) using the best-fitting substitution model on the T-REX Web server (Boc *et al.* 2012). One thousand bootstraps were carried out. A Bayesian reconstruction of the data matrix was performed with MrBayes v3.0b4 (Ronquist & Huelsenbeck 2003) using the best-fitting substitution model. Four Markov chain Monte Carlo chains ran for 2 million generations, sampling every 1000 generations with a burn-in of 10%. A majority rule consensus tree was created to examine the posterior probabilities of each clade.

RESULTS

Both theca and cyst morphology of 11 diplopsalioidean species (species listed in Tables 1, 2, with authorities) from China were subjected to detailed morphological examination. The cyst–theca relationships of four of these species (*Boreadinium breve*, *Diplopsalopsis ovata*, *Niea chinensis*, *Oblea torta*) have not been reported before. These species carried a pronounced left sulcal list that often masked the left sulcal plate with the cell shape ranging from globular to lenticular. A new genus, *Niea* T. Liu, K.N. Mertens & H. Gu, was erected to encompass species with the plate tabulation Po, X, 3′, 1a, 6″, 3C+t, ?4S, 5‴, 2⁗ and an ortho-type 1′. In addition, *Diplopsalis lebouriae* was transferred to a second new genus, *Qia* T. Liu, K.N. Mertens & H. Gu. As a consequence, the genera *Oblea* and *Diplopsalis* were emended accordingly.

Molecular phylogeny

Twenty-two new LSU rDNA sequences were obtained from 11 diplopsalioideans species (Table 2). For intraspecific comparisons, Chinese *D. lenticula* type A differed from type B for 32 positions (94.99% similarity), and they differed from *D. lenticula* from the Gulf of Mexico (EF152783) for 19 and 46 nucleotides, respectively (97.03% and 96.70% similarity); two cells of *Diplopsalo. ovata* differed from each other for 57 positions (95.93% similarity), and two cells of *Lebouraia pusilla* differed from each other for 6 bp (99.57%). Three cells of *N. chinensis* differed from each other at 11 positions (99.22% similarity), and three cells of *Niea acanthocysta* differed from each other at four positions (99.90% similarity). *Qia lebouriae* type A differed from type B at 49 positions (96.63% similarity). Two cells of *B. breve* shared identical sequences, and they differed from *O. rotunda* at 26 positions (98.13% similarity).

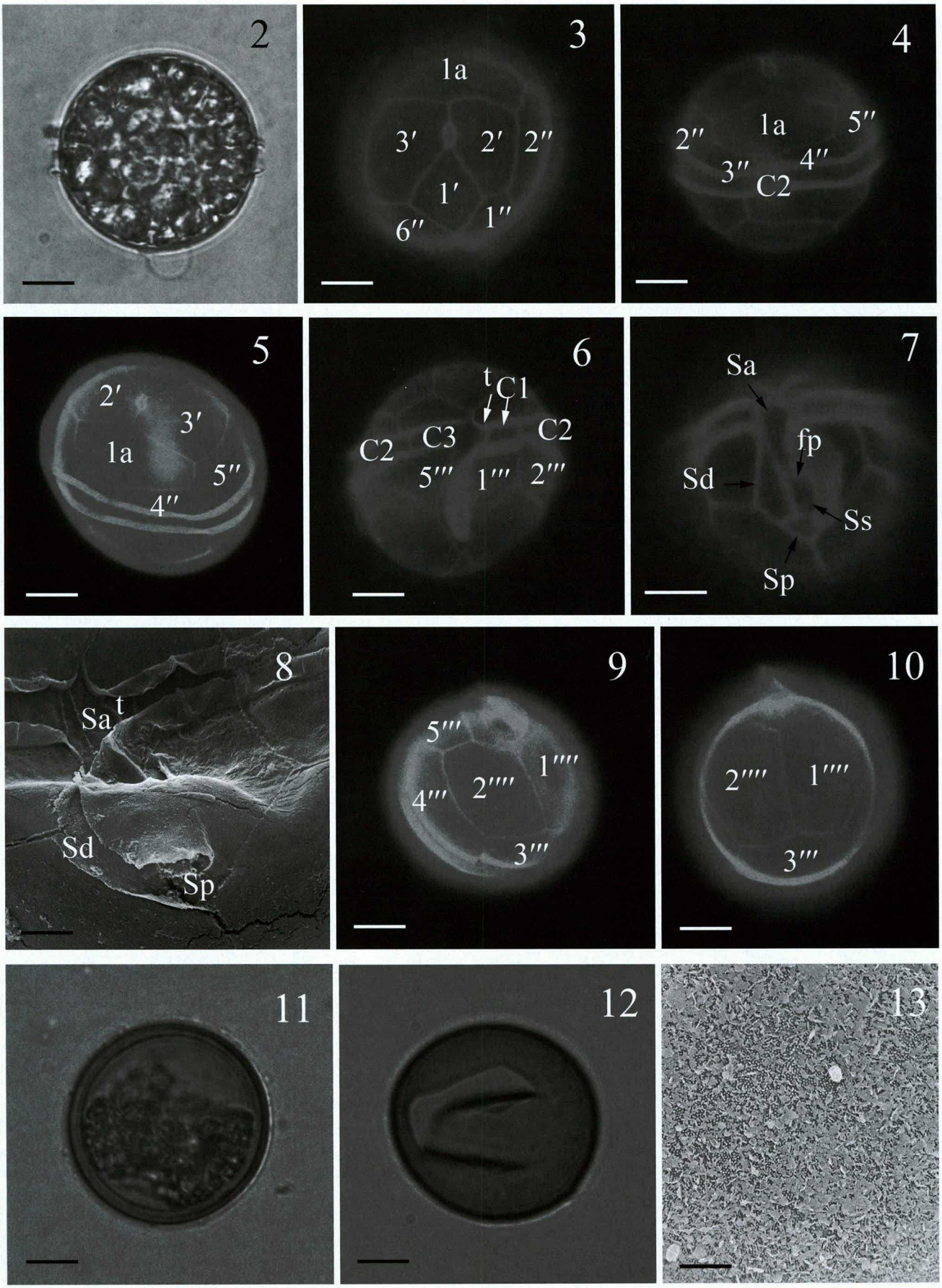
2
3
1a
3′
2′
2″
1′
6″
1″
4
2″
1a
5″
3″
4″
C2
5
2′
3′
1a
5″
4″
6
t
C1
C2
C3
C2
5‴
1‴
2‴
7
Sa
fp
Sd
Ss
Sp
8
Sa
t
Sd
Sp
9
5‴
1⁗
4‴
2⁗
3‴
10
2⁗
1⁗
3‴
11
12
13

The best phylogenetic tree constructed by Bayesian inference (BI) is illustrated in Fig. 1. The tree generated with maximum likelihood (ML) was nearly identical (Fig. S2). Three clades (*Protoperidinium sensu stricto*, *Oceanica* and *Monovela*) were well resolved, but the subfamily Diplopsalioideae was polyphyletic and consisted of three subclades. Clade *Diplopsalioideae* I comprised species of *Diplopsalis*, *Oblea*, *Boreadinium* and *Lebouraia* with low support (BI posterior probability: 0.54/ML bootstrap: 20); clade *Diplopsalioideae* II comprised only species of *Preperidinium*, with maximal support (BI posterior probability: 1.00/ML bootstrap: 100) and clade *Diplopsalioideae* III comprised species of *Niea*, *Diplopelta*, *Gotoius*, *Qia* and *Diplopsalopsis* with maximal support. Clades *Diplopsalioideae* II and III group together with the *Oceanica* clade with strong support (BI posterior probability: 0.92/ML bootstrap: 100).

Niea T. Liu, K.N. Mertens & H. Gu *gen. nov.*

DIAGNOSIS: Plate tabulation = Po, X, 3′, 1a, 6″, 3C+t, ?4S, 5‴, 2⁗. The first apical plate (1′) quadrangular (ortho-type). The posterior sulcal plate (Sp) small and of Caspica-type. The genus *Niea* differs from *Oblea* in an ortho 1′ and configuration of 1a plate.

TYPE SPECIES: *Niea chinensis* T. Liu, K.N. Mertens & H. Gu.

ETYMOLOGY: '*Niea*' is derived from Dashu Nie, a Chinese researcher who carried out pioneering work on dinoflagellate taxonomy, particularly on the diplopsalioideans.

Niea chinensis T. Liu, K.N. Mertens & H. Gu *sp. nov.* Figs 2–19

DESCRIPTION: Motile cells spherical with a diameter of 25.0–47.0 μm. The plate tabulation = Po, X, 3′, 1a, 6″, 3C+t, ?4S, 5‴, 2⁗. The first apical plate (1′) rhombic (ortho-type). Plate 1a hexagonal and in the middle of the dorsal epitheca. The posterior sulcal (Sp) plate small and of Caspica-type. Cysts subspherical and smooth with a diameter of 25.0–50.0 μm. The archeopyle theropylic corresponding to 1a plate.

HOLOTYPE: Specimen TIO2014PER03, a SEM stub, deposited at Third Institute of Oceanography, SOA, Xiamen 361005, China.

TYPE LOCALITY: South China Sea (21°29.97″N, 108°13.87″E), close to Bailong (Fangchenggang, Guangxi province, China).

ETYMOLOGY: '*chinensis*' is derived from China and refers to the wide geographic area along the Chinese coast where the species was recorded.

GENBANK ACCESSION NUMBERS: KP702720, KP702721 and KP702722; the nuclear-encoded LSU rRNA gene sequence of the vegetative stage.

The vegetative cells were spherical, contained lipid bodies and were pale green (Fig. 2). The plate formula was Po, X, 3′, 1a, 6″, 3C+t,?4S, 5‴, 2⁗. The first apical plate (1′) was rhombic (ortho-type); whereas, plates 2′ and 3′ were pentagonal (Fig. 3). There was only one hexagonal anterior intercalary plate (1a) located in the middle of the dorsal epitheca (Fig. 4). Among the six precingular plates, plates 2″ and 5″ were pentagonal; whereas, the others were four-sided (Figs 3–6). The cingulum slightly ascended and had a short cingular list without ribs (Fig. 6). We were unable to verify the exact number of sulcal plates. The cells had an A type of the anterior sulcal (Sa) plate *sensu* Dodge & Hermes (1981). The left sulcal (Ss) plate was long and narrow, sheltered by a large list on the left of the sulcus; there was an elliptical flagellar pore between Sa, Sd (the right sulcal plate), Ss and Sp plates (Fig. 7). The posterior sulcal (Sp) plate was small and of the Caspica-type (Figs 7, 8). The five postcingular plates were four-sided except that plate 3‴ was pentagonal (Figs 7, 9, 10). There were two five-sided antapical plates of almost equal size (Fig. 10). The spherical cyst was brown in color and smooth-walled (Fig. 11). The archeopyle was hexagonal and theropylic, corresponding to 1a plate (Fig. 12). The cyst surface was microgranulate (Fig. 13). The plate pattern of *N. chinensis* is illustrated in Figs 14–19.

The incubated motile cells were 25.0 (38.3) 47.0 μm in diameter (n = 20), and the cysts germinated to give identifiable thecae 25.0 (39.3) 50.0 μm in diameter (n = 20).

Niea acanthocysta (Kawami, Iwataki & Matsuoka) T. Liu, K.N. Mertens & H. Gu *comb. nov.* Figs 20–25

BASIONYM: *Oblea acanthocysta* Kawami, Iwataki & Matsuoka [2006; *Plankton and Benthos Research* 1(4), pp. 183–190, figs 1, 2].

Based upon the Chinese material examined here, the vegetative cells were subspherical, contained lipid bodies and were pale green (Fig. 20). The plate formula was Po, X, 3′, 1a, 3C+t, 6″, ?4S, 5‴, 2⁗. The first apical plate (1′) was rhombic (ortho-type); whereas, plates 2′ and 3′ were pentagonal (Figs 21, 22). There was only one hexagonal anterior intercalary plate slightly inclined to the left of the

←

Figs 2–13. LM and SEM of vegetative cells and cysts of *N. chinensis*. Cell in Figs 2–4, 6 was used for sequencing.
Fig. 2. A living cell in ventral view showing the globular shape (LM). Scale bar = 10 μm.
Fig. 3. A calcofluor-stained cell in apical view, showing three apical plates (1′–3′) (LM). Scale bar = 10 μm.
Figs 4, 5. Calcofluor-stained cells in dorsal view, showing the anterior intercalary plate (1a) (LM). Scale bar = 10 μm.
Fig. 6. A calcofluor-stained cell in ventral view showing three cingular plates (C1–C3), the transitional plate (t) and a prominent sulcal list (LM). Scale bar = 10 μm.
Fig. 7. A calcofluor-stained cell in ventral view, showing an anterior sulcal plate (Sa), a left sulcal plate (Ss), the flagellar pore (fp), a right sulcal plate (Sd) and a posterior sulcal plate (Sp) (LM). Scale bar = 10 μm.
Fig. 8. Detail of the sulcal area showing the arrangement between Sa, Sd and transitional plate (t) (SEM). Scale bar = 5 μm.
Figs 9, 10. Calcofluor-stained cells in antapical view showing five postcingular plates (1‴–5‴) and two antapical plates (1⁗, 2⁗) (LM). Scale bar = 10 μm.
Fig. 11. A living cyst full of granules (LM). Scale bar = 10 μm.
Fig. 12. An empty cyst showing the archeopyle (LM). Scale bar = 10 μm.
Fig. 13. Detail of the cyst surface showing the granules (SEM). Scale bar = 5 μm.

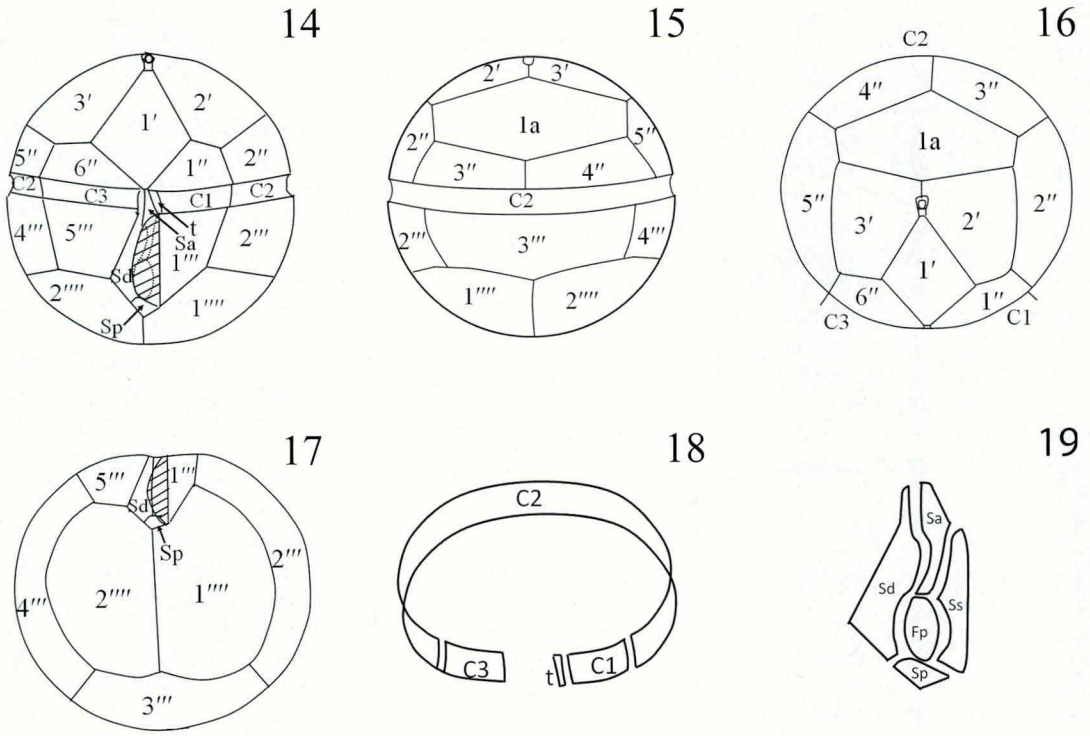

Figs 14–19. Interpreted tabulation of motile stage of *N. chinensis*.
Fig. 14. Ventral view.
Fig. 15. Dorsal view.
Fig. 16. Apical view.
Fig. 17. Antapical view.
Fig. 18. Cingular plates.
Fig. 19. Sulcal plates (Sa, anterior sulcal plate; Ss, left sulcal plate; Sd, right sulcal plate; Sp, posterior sulcal plate).

dorsal epitheca (Fig. 22). Among the six precingular plates, plates 2″ and 5″ were pentagonal; whereas, the others were four-sided (Figs 21, 22). The cingulum slightly ascended and had a short cingular list without ribs (Figs 21, 23). The five postcingular plates were four-sided except that plate 3‴ was pentagonal (Figs 23, 24). We were unable to verify the exact number of sulcal plates because of the prominent left sulcal list. The cells had an A type of Sa plate *sensu* Dodge & Hermes (1981). The Sp plate was small and of the Caspica-type. There were two five-sided antapical plates of almost equal size (Fig. 24). The spherical cyst was pale brown in color with a microgranular wall and ornamented with many solid, erect or curved spines with a length of 6.0 (8.2) 10.4 μm ($n = 7$; Fig. 25). The archeopyle was theropylic (Fig. 25).

The incubated motile cells were 32.0 (38.0) 42.0 μm in length and 35.0 (41.3) 45.0 μm in width ($n = 4$). Cysts germinated to give identifiable thecae with a diameter of 37.0 (40.3) 45.0 μm ($n = 7$).

Niea torta (Abé) T. Liu, K.N. Mertens & H. Gu *comb. nov.*
Figs 26–34

BASIONYM: *Diplopsalis torta* Abé (1941; *Records of Oceanographic Works in Japan* 12, pp. 121–144, figs 1–6).

HOMOTYPIC SYNONYMS: *Oblea torta* (Abé) Balech *ex* Sournia 1973, p. 49; *Dissodium tortum* (Abé) Dodge & Hermes 1981, p. 22.

HETEROTYPIC SYNONYMS: *Diplopsalis hainanensis* Nie 1943, p. 13, figs 20–25; *Peridiniopsis hainanensis* (Nie) Taylor 1976, p. 131.

Based upon the Chinese material examined here, the vegetative cells were subspherical, contained lipid bodies and were pale green (Fig. 26). The plate formula was Po, X, 3′, 1a, 3C+t, 6″, ?4S, 5‴, 2⁗. The first apical plate (1′) was rhombic (ortho-type); whereas, plates 2′ and 3′ were pentagonal (Figs 27, 28). There was only one hexagonal anterior intercalary plate displaced to the left dorsal side (Figs 27, 29). Among the six precingular plates, plates 2″ and 5″ were pentagonal; whereas, the others were four-sided (Figs 27–29). The cingulum was circular without displacement and had pronounced cingular list without ribs. The five post-cingular plates were four-sided except that plate 3‴ was pentagonal (Figs 30, 31). We were unable to verify the exact number of sulcal plates because of the prominent left sulcal list. The cells had an A type of anterior sulcal (Sa) plate *sensu* Dodge & Hermes (1981). The Ss plate was subrectangular. The Sp plate was small and of the Caspica-type (Fig. 30). There were two five-sided antapical plates of almost equal size (Fig. 31). The spherical cyst was brown in color and smooth without ornamentation (Figs 32, 33). The archeopyle was theropylic epicystal, formed by a slit along the cingulum (Fig. 34).

The incubated motile cells were 50.0 (57.5) 65.0 μm in length and 60.0 (67.5) 75.0 μm in width ($n = 2$). Cysts gave

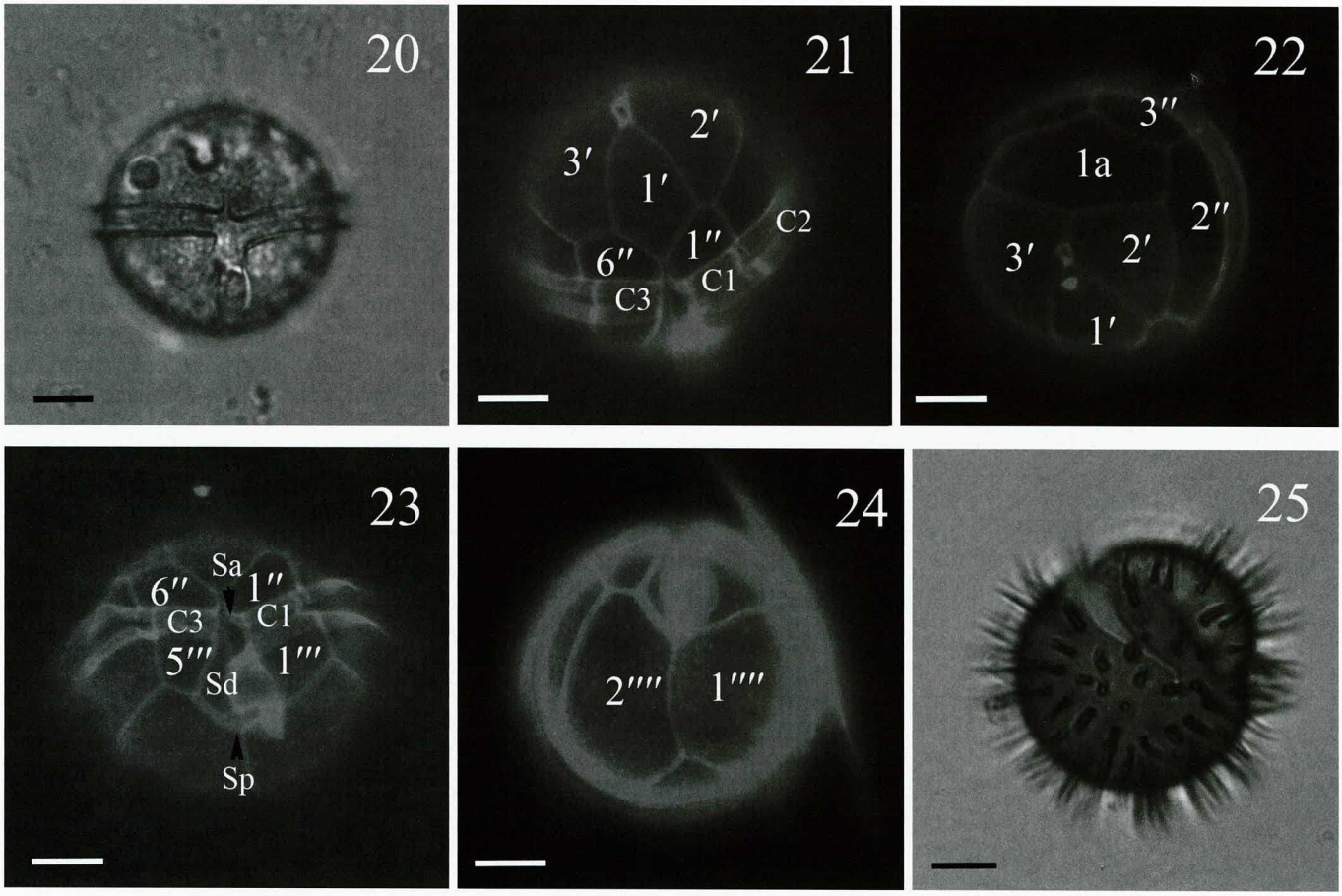

Figs 20–25. LM of vegetative cells and cysts of *N. acanthocysta*. Cell in Figs 20–24 was used for sequencing. Scale bars = 10 μm.
Fig. 20. A living cell in ventral view showing the subspherical shape.
Fig. 21. A calcofluor-stained cell in ventral view showing the first apical plate (1′) and three cingular plates (C1–C3).
Fig. 22. A calcofluor-stained cell in apical view, showing three apical plates (1′–3′) and the anterior intercalary plate (1a).
Fig. 23. A calcofluor-stained cell in ventral view, showing an anterior sulcal plate (Sa), a prominent sulcal list, a right sulcal plate (Sd) and a posterior sulcal plate (Sp).
Fig. 24. A calcofluor-stained cell in antapical view showing five postcingular plates (1‴–5‴) and two antapical plates (1⁗, 2⁗).
Fig. 25. An empty cyst showing the archeopyle.

rise to identified thecae with diameters of 60.0 (65.0) 70.0 μm ($n = 2$).

Qia T. Liu, K.N. Mertens & H. Gu *gen. nov*

DIAGNOSIS: Plate tabulation = Po, X, 3′, 1a, 6″, 3C+t, ?4S, 5‴, 1⁗. The first apical plate (1′) rhombic (ortho-type). The anterior intercalary plate (1a) hexagonal, located in the middle of the dorsal epitheca. The posterior sulcal (Sp) plate small and of Caspica-type. The genus *Qia* differs from *Diplopsalis* in the configuration of 1a plate.

TYPE SPECIES: *Qia lebouriae* (Nie) *comb. nov.*

BASIONYM: *Diplopsalis lenticula* var. *lebourii* Nie (1943; *Sinensia* 14, pp. 1–21, figs 14–19).

SYNONYM: *Diplopsalis lebouriae* (Nie) Balech 1967, p. 12.

ETYMOLOGY: '*Qia*' is derived from Yuzao Qi, a Chinese researcher who carried out pioneering work on harmful algal blooms.

Qia lebouriae (Nie) T. Liu, K.N. Mertens & H. Gu *comb. nov.*
Figs 35–46

Two morphotypes of cysts (type A and type B) produced cells fitting the description of *Q. lebouriae*. Motile cells from cyst type A were subspherical (Fig. 35). The plate tabulation was Po, X, 3′, 1a, 3C+t, 6″, ?4S, 5‴, 1⁗. The first apical plate (1′) was rhombic (ortho-type) and wide; whereas, plates 2′ and 3′ were pentagonal (Fig. 36). There was only one hexagonal anterior intercalary plate located in the middle of the dorsal epitheca (Fig. 37). Among the six precingular plates, plates 2″ and 5″ were pentagonal; whereas, the others were four-sided (Figs 36–38). The cingulum slightly ascended (Fig. 35). We were unable to verify the exact number of sulcal plates because of the prominent left sulcal list (Fig. 35). The cells had an A type of the Sa plate *sensu* Dodge & Hermes (1981; Fig. 35). The Sp plate was small and of the Caspica-type (Fig. 39). There were five four-sided postcingular plates and one large antapical plate (Fig. 39). Cysts of

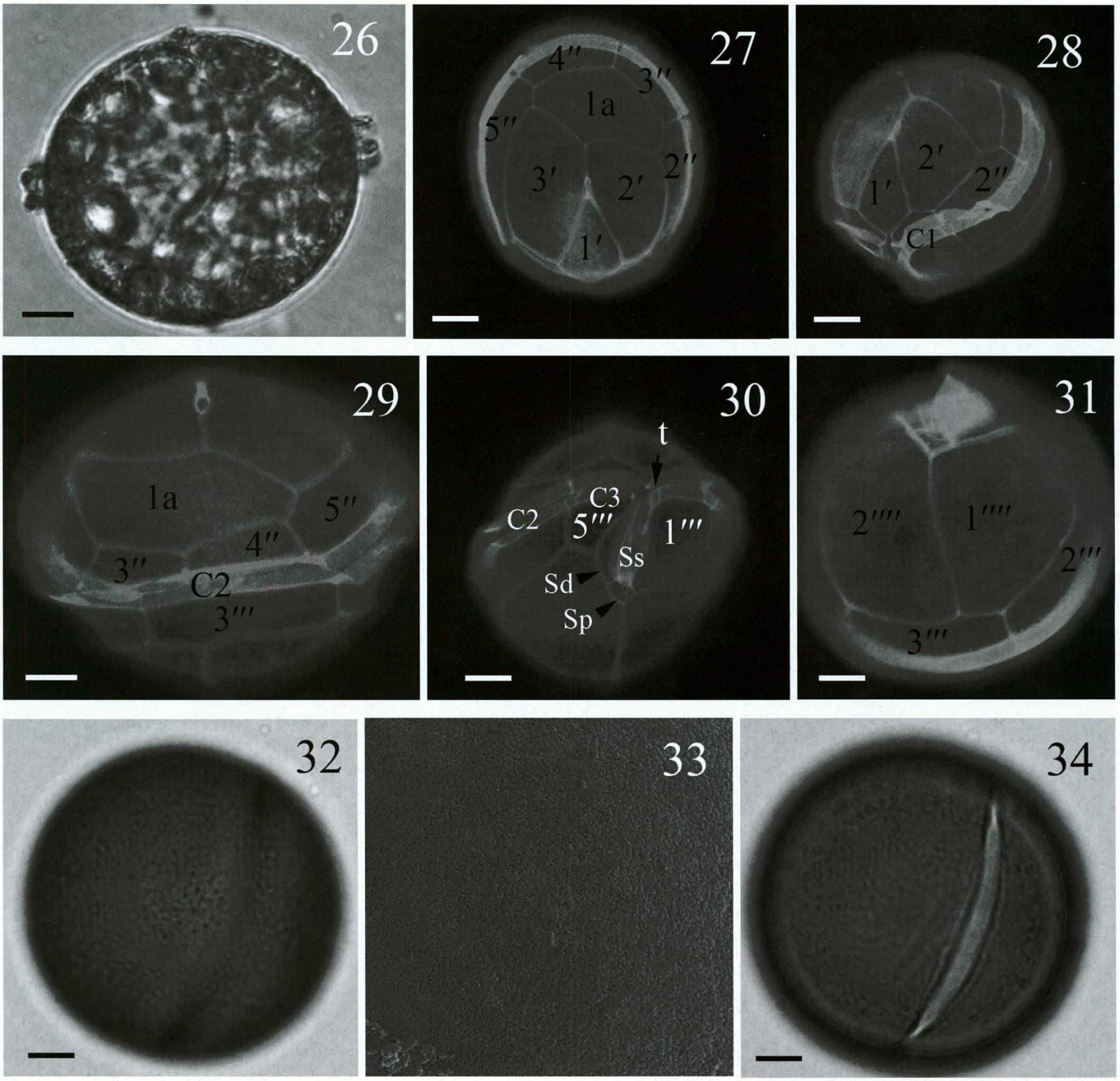

Figs 26–34. LM and SEM of vegetative cells and cysts of *N. torta*. Cell in Figs 26, 29, 31 was incubated from cyst in Fig. 34 and used for sequencing. Scale bars = 10 μm.

Fig. 26. A living cell in ventral view showing the lenticular shape (LM).

Fig. 27. A calcofluor-stained cell in apical view, showing three apical plates (1′–3′), one anterior intercalary plate (1a) and six precingular plates (1″–6″) (LM).

Fig. 28. A calcofluor-stained cell in left lateral view, showing the ortho-1′ and the first cingular plate (C1) (LM).

Fig. 29. A calcofluor-stained cell in dorsal view, showing the six-sided 1a plate displaced to the left (LM).

Fig. 30. A calcofluor-stained cell in ventral view showing two cingular plates (C2, C3), the transitional plate (t), a prominent sulcal list, a right sulcal plate (Sd), a left sulcal plate (Ss) and a small posterior sulcal plate (Sp) (LM).

Fig. 31. A calcofluor-stained cell in antapical view showing five postcingular plates (1‴–5‴) and two antapical plates (1⁗, 2⁗) (LM).

Fig. 32. An empty cyst with smooth surface (LM).

Fig. 33. Detail of the cyst surface (SEM).

Fig. 34. An empty cyst showing the theropylic epicystal archeopyle (LM).

type A were spherical and brown, covered with numerous short hairs with a length of 3.1 (3.4) 3.8 μm ($n = 3$; Fig. 40). The archeopyle was theropylic and corresponded to plate 1a.

Cells generated from cyst type B were nearly identical to those from cyst type A except that the first apical plate was relatively narrow (Figs 41–44). Cysts of type B were spherical and brown, covered with numerous solid spines with a length of 6.3 (8.3) 10.0 μm ($n = 7$; Fig. 45). The archeopyle was hexagonal and theropylic, corresponding to plate 1a (Fig. 46).

Dimensions: Type A of incubated motile cells: 47.0 (49.6) 52.2 μm in length, 50.0 (55.0) 60.0 μm in width ($n = 2$). Cysts gave rise to identified thecae: 50.0 (56.7) 60.0 μm in diameter ($n = 3$). Type B of incubated motile cells: 47.9 (49.9) 51.5 μm in length, 55.0 (57.6) 60.0 μm in width ($n = 4$). Cysts gave rise to identified thecae: 45.0 (51.7) 60.0 μm in diameter ($n = 7$).

Boreadinium J.D. Dodge & H.B. Hermes
Boreadinium breve (Abé) Sournia

Based upon the Chinese material examined here, the motile cells were more or less spherical. The cells contained lipid bodies and were pale greenish (Fig. 47). The plate tabulation was Po, X, 4′, 1a, 6″, 3C+t, ?3S, 5‴, 1⁗. The first apical plate (1′) was five-sided (meta-type; Fig. 48). Plates 2′ and 3′ were small; whereas, plate 4′ was five-sided and large. There was only one anterior intercalary plate which contacted plates 1″–5″ (Figs 48–50). Among the six precingular plates, plate 5″ was five-sided; whereas, the other plates were four-sided. The cingulum was circular, without displacement, and had a short cingular list with ribs (Figs 48, 51). We were unable to verify the exact number of sulcal plates because of the prominent left sulcal list. The cells had a B type of Sa plate *sensu* Dodge & Hermes (1981). The Sp plate was small and of the Caspica-type (Figs 51, 52). There was an elliptical flagellar pore located between Sa, Sd and Sp (Fig. 51). There were five four-sided postcingular plates and one large antapical plate (Fig. 52). One cell with three apical plates was observed (Fig. 53). The cyst was oval and pale brown with a coarsely granular surface, sometimes with mucus (Fig. 54). The archeopyle was large and theropylic, possibly corresponding to plate 1a (Fig. 55).

The incubated motile cells were 30.0 (35.0) 40.0 μm in diameter ($n = 5$). Cysts gave rise to identified thecae 30.0 (35.0) 40.0 μm in diameter ($n = 5$).

Diplopelta F. Stein *ex* E. Jørgensen
Diplopelta globula (Abé) Balech

Based upon the Chinese material examined here, the motile cells were subspherical. The cell contents were pale greenish (Fig. 56). The plate tabulation was Po, 3′, 2a, 3C+t, 6″, ?3S, 5‴, 2⁗ (Figs 57–62). There was a small apical pore without a canal plate (Fig. 58). The first apical plate (1′) was rhombic (ortho-type; Figs 57, 58). Plate 2′ was six-sided and slightly larger than the five-sided 3′ plate (Fig. 57). Plate 1a was small and diamond-shaped; whereas, plate 2a was large and hexagonal (Fig. 59). Among the six precingular plates, plates 2″, 3″ and 5″ were pentagonal; whereas, the others were four-sided (Figs 57–60). The cingulum was circular without displacement (Fig. 61). We were unable to verify the exact number of sulcal plates because of the prominent left sulcal list (Fig. 61). The cells had an A type of the Sa plate *sensu* Dodge & Hermes (1981), and the Sp plate was medium sized and of the Asymmetrica-type (Fig. 61). The postcingular plates were four-sided except that plate 3‴ was pentagonal (Figs 61, 62). There were two five-sided antapical plates of similar size (Fig. 62). The spherical cyst was dark brown (Fig. 63). The archeopyle was large and theropylic and corresponded to plate 2a (Fig. 64).

The incubated motile cell was 60.0 μm in length and 70.9 μm in width ($n = 1$). Cysts germinated to give identifiable thecae 60.0 μm in diameter ($n = 1$).

Diplopsalis (Bergh) emend

Emended diagnosis: Plate tabulation = Po, X, 3′, 1a, 6″, 3C+t, ?4S, 5‴, 1⁗. The first apical plate (1′) quadrangular (ortho-type). The anterior intercalary plate (1a) rectangular, located in the low part of the dorsal epitheca. The posterior sulcal (Sp) plate small and of Caspica-type. The genus *Diplopsalis* differs from *Qia* in the configuration of the 1a plate.

TYPE SPECIES: *Diplopsalis lenticula* Bergh.

Diplopsalis lenticula Bergh

Based upon the Chinese material examined here, the motile cells of type A were lenticular in shape with a pronounced apical horn (Fig. 65). The plate tabulation was Po, X, 3′, 1a, 3C+t, 6″, ?4S, 5‴, 1⁗. The first apical plate (1′) was quadrangular (ortho-type); whereas, plates 2′ and 3′ were five-sided with 3′ much larger than 2′ (Figs 66, 67). There was one rectangular and curved anterior intercalary plate slightly displaced to the left of the epitheca (Figs 67, 68). Among the six precingular plates, plates 2″ and 5″ were pentagonal; whereas, the others were four-sided. The cingulum did not show displacement (Fig. 69). We were unable to verify the exact number of sulcal plates because of the prominent left sulcal list. The cells had an A type of the Sa plate *sensu* Dodge & Hermes (1981; Figs 69, 70). The Sp plate was small and of the Caspica-type (Fig. 70). The postcingular plates were four-sided with plates 1‴ and 5‴ much smaller (Fig. 71). There was only one irregular antapical plate (1⁗; Fig. 71). The motile cells of type B were identical to those of type A except that its 2′ and 3′ were equal in size (Fig. 72). Cysts producing both types of motile cells were identical in morphology. They were spherical and pale brown with smooth or sometimes coarse surface. The archeopyle was theropylic and corresponded to suturing along predetermined plate boundaries (Fig. 73).

Dimensions: Type A of incubated motile cells was 45.0 (48.3) 50.0 μm in width, 35.0 (36.7) 38.0 μm in length ($n = 3$). Cysts germinated to give identifiable thecae 35.0 (42.5) 50.0 μm in diameter ($n = 8$). Type B of incubated motile cells was 35.0 μm in width, 26.6 μm in length ($n = 1$). Cysts germinated to give identifiable thecae 30.0 (32.5) 35.0 μm in diameter ($n = 2$).

Diplopsalopsis A. Meunier
Diplopsalopsis ovata (Abé) J.D. Dodge & Toriumi

Based upon the Chinese material examined here, the motile cells were subspherical. The cells contained lipid bodies and were pale green (Fig. 74). The plate tabulation was Po, X, 3′, 2a, 3C+t, 7″, ?3S, 5‴, 2⁗ (Figs 75–80). The first apical plate (1′) was quadrangular (ortho-type); whereas, plate 2′

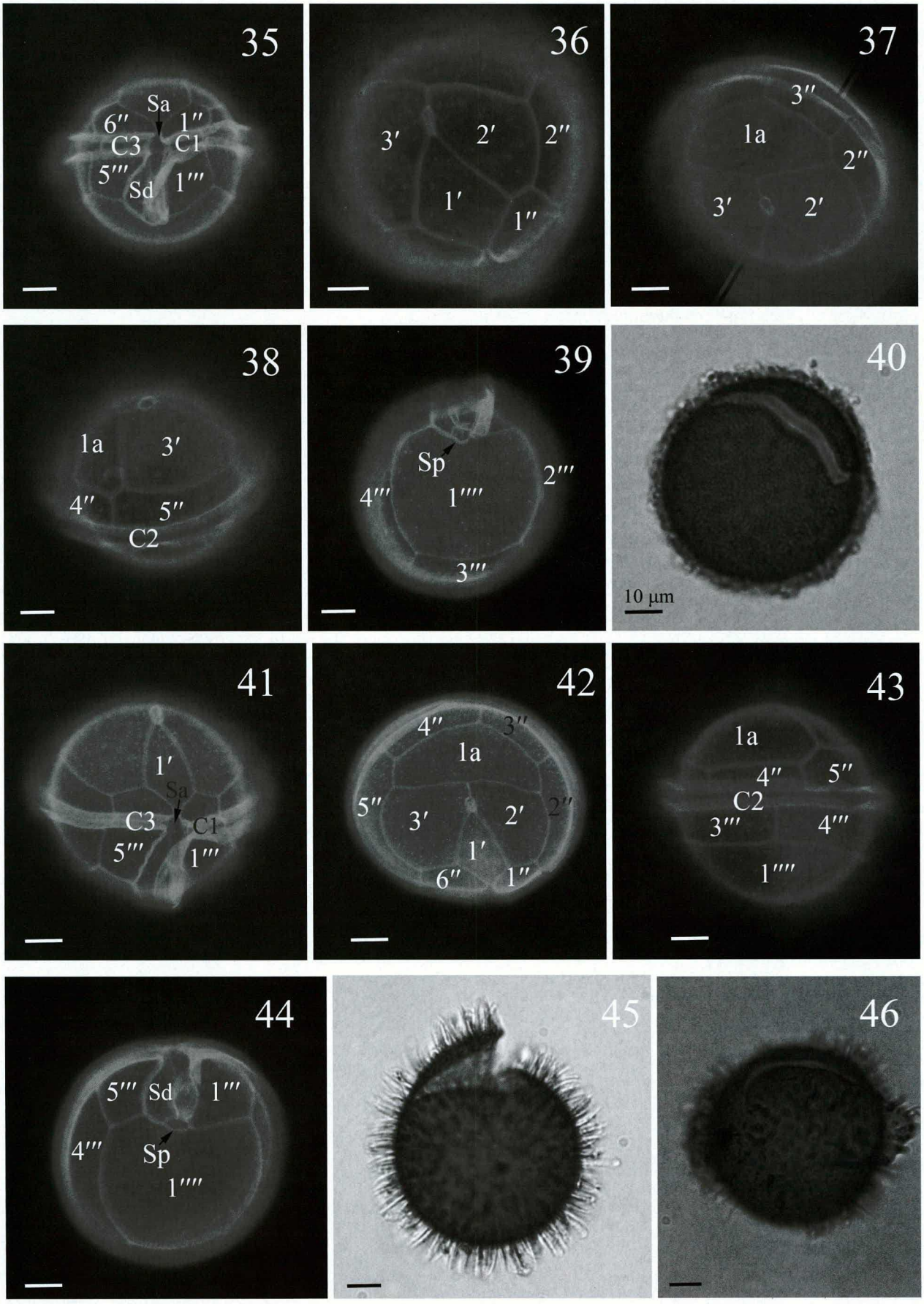
35
Sa
6″
1″
C3
C1
5‴
Sd
1‴
36
3′
2′
2″
1′
1″
37
3″
1a
2″
3′
2′
38
1a
3′
4″
5″
C2
39
Sp
2‴
4‴
1⁗
3‴
40
10 µm
41
1′
Sa
C3
C1
5‴
1‴
42
4″
3″
1a
5″
3′
2′
2″
1′
6″
1″
43
1a
4″
5″
C2
3‴
4‴
1⁗
44
5‴
Sd
1‴
4‴
Sp
1⁗
45
46

was six-sided and similar in size to the five-sided 3′ plate (Fig. 75). The six-sided 2a plate was slightly larger than the five-sided 1a plate (Figs 76, 77). Among the seven precingular plates, plates 4″ and 6″ were pentagonal; whereas, the others were four-sided (Figs 75–77). The cingulum was circular without displacement (Fig. 78). The five postcingular plates were four-sided, except that plate 3‴ was pentagonal (Figs 79, 80). The two antapical plates were similar in size (Fig. 80). We were unable to verify the exact number of sulcal plates because of the prominent left sulcal list. The cells had an A type of the Sa plate *sensu* Dodge & Hermes (1981), and the Sp plate was of the Asymmetrica-type (Fig. 78).

Cysts were spherical, brown and smooth-walled (Fig. 81). The archeopyle was hexagonal and theropylic, corresponding to 2a plate (Fig. 81). Two flagellar scars were present (Fig. 82).

The incubated motile cells were 36.0 (46.6) 58.0 μm in width and 33.0 (41.3) 50.0 μm in length ($n = 8$). Cysts germinated to give identifiable thecae with diameters of 40.0 (45.7) 50.0 μm ($n = 11$).

Lebouraia T. H. Abé *ex* Sournia
Lebouraia pusilla (Balech & Akselman) J.D. Dodge & Toriumi

Based upon the Chinese material examined here, the motile cells were globular, full of lipid bodies and pale greenish (Fig. 83). The plate tabulation was Po, X, 3′, 2a, 3C+t, 6″, ?3S, 5‴, 2⁗. The first apical plate (1′) was meta-type (Fig. 84); whereas, plates 2′ and 3′ were four- and six-sided, respectively (Fig. 85). Plate 1a was six-sided and markedly larger than the four-sided 2a plate (Figs 86, 87). Among the six precingular plates, plates 1″ and 3″ were four-sided; whereas, plates 4″–6″ were pentagonal and plate 2″ was six-sided (Figs 84–87). The cingulum did not show displacement (Fig. 88). We were unable to verify the exact number of sulcal plates because of the prominent left sulcal list. The cells had an A type of Sa plate *sensu* Dodge & Hermes (1981), and the Sp plate was small and of the Caspica-type (Figs 88, 89). The postcingular plates were four-sided except that plate 3‴ was five-sided (Figs 87–89). The two antapical plates were five-sided and similar in size (Fig. 89). The spherical cyst was pale brown and full of granules (Fig. 90). The archeopyle was hexagonal and theropylic and corresponded to plate 1a (Fig. 91).

The incubated motile cells were 30.0 (33.5) 40.0 μm in diameter ($n = 11$). Cysts germinated to give identifiable thecae with diameters of 30.0 (36.6) 40.0 μm ($n = 11$).

Oblea (Balech) emend

Emended diagnosis: Plate tabulation = Po, X, 3′, 1a, 6″, 3C+t, 5‴, 2⁗. The first apical plate (1′) is of meta-type. Plate 1a is very large. The genus *Oblea* differs from *Niea* in the meta 1′ and configuration of 1a plate.

TYPE SPECIES: *Oblea baculifera* Balech *ex* Loeblich Jr. & Loeblich III.

Oblea rotunda (Lebour) Balech *ex* Sournia

Based upon the Chinese material examined here, the motile cells were more or less spherical. The cells contained lipid bodies and were pale greenish (Fig. 92). The plate tabulation was Po, X, 3′, 1a, 3C+t, 6″, ?4S, 5‴, 2⁗. The first apical plate (1′) was of meta-type (Figs 93, 94). Plate 2′ was fan-shaped and much smaller than plate 3′ (Fig. 95). There was one large anterior intercalary plate that contacted plates 1″–5″ (Figs 94, 96, 97). Among the six precingular plates, plate 5″ was five-sided; whereas, the others were four-sided. The cingulum was circular, without displacement and had a short cingular list with ribs (Fig. 94). We were unable to verify the exact number of sulcal plates because of the prominent left sulcal list. The cells had a C type of Sa plate *sensu* Dodge & Hermes (1981). The Ss plate was narrow and J-shaped. The Sp plate was small and of the Caspica-type (Figs 98, 99). The postcingular plates were four-sided, except that plate 3‴ was pentagonal (Fig. 99). There were two pentagonal antapical plates with the first one much smaller (Fig. 99). Cysts were spherical and pale brown and covered with mucus (Fig. 100). The archeopyle was large and theropylic intercalary and corresponded to plate 1a (Fig. 100).

The incubated motile cells were 21.0 (21.5) 21.9 μm in length and 22.5 (23.3) 24.0 μm in width ($n = 2$). Cysts gave rise to identified thecae with diameters of 25.0 (30.0) 35.0 μm ($n = 6$).

←

Figs 35–46. LM of vegetative cells and cysts of *Q. lebouriae*. The cell in Figs 35–39 was incubated from cyst in Fig. 40 (cyst type A) and used for sequencing. The cell in Figs 41–44 were incubated from cyst in Figs 45, 46 (cyst type B) and used for sequencing. Scale bars = 10 μm.

Fig. 35. A calcofluor-stained cell in ventral view showing two cingular plates (C1, C3), a prominent sulcal list, an anterior sulcal plate (Sa) and a right sulcal plate (Sd).

Figs 36, 37. Calcofluor-stained cells in apical view, showing three apical plates (1′–3′) and the anterior intercalary plate (1a).

Fig. 38. A calcofluor-stained cell in dorsal view, showing the second cingular plate (C2).

Fig. 39. A calcofluor-stained cell in antapical view showing five postcingular plates (1‴–5‴), one antapical plate (1⁗) and a small posterior sulcal (Sp) plate.

Fig. 40. An empty cyst with short hairs showing the archeopyle.

Fig. 41. A calcofluor-stained cell in ventral view showing an ortho-type 1′, two cingular plates (C1, C3), a prominent sulcal list and an anterior sulcal plate (Sa).

Fig. 42. A calcofluor-stained cell in apical view, showing three apical plates (1′–3′), one anterior intercalary plate (1a) and six precingular plates (1″–6″).

Fig. 43. A calcofluor-stained cell in dorsal view showing the second cingular plate (C2).

Fig. 44. A calcofluor-stained cell in antapical view, showing the large antapical plate (1⁗) and a small posterior sulcal plate (Sp).

Fig. 45. An empty cyst showing the long, hollow spines.

Fig. 46. An empty cyst showing the archeopyle.

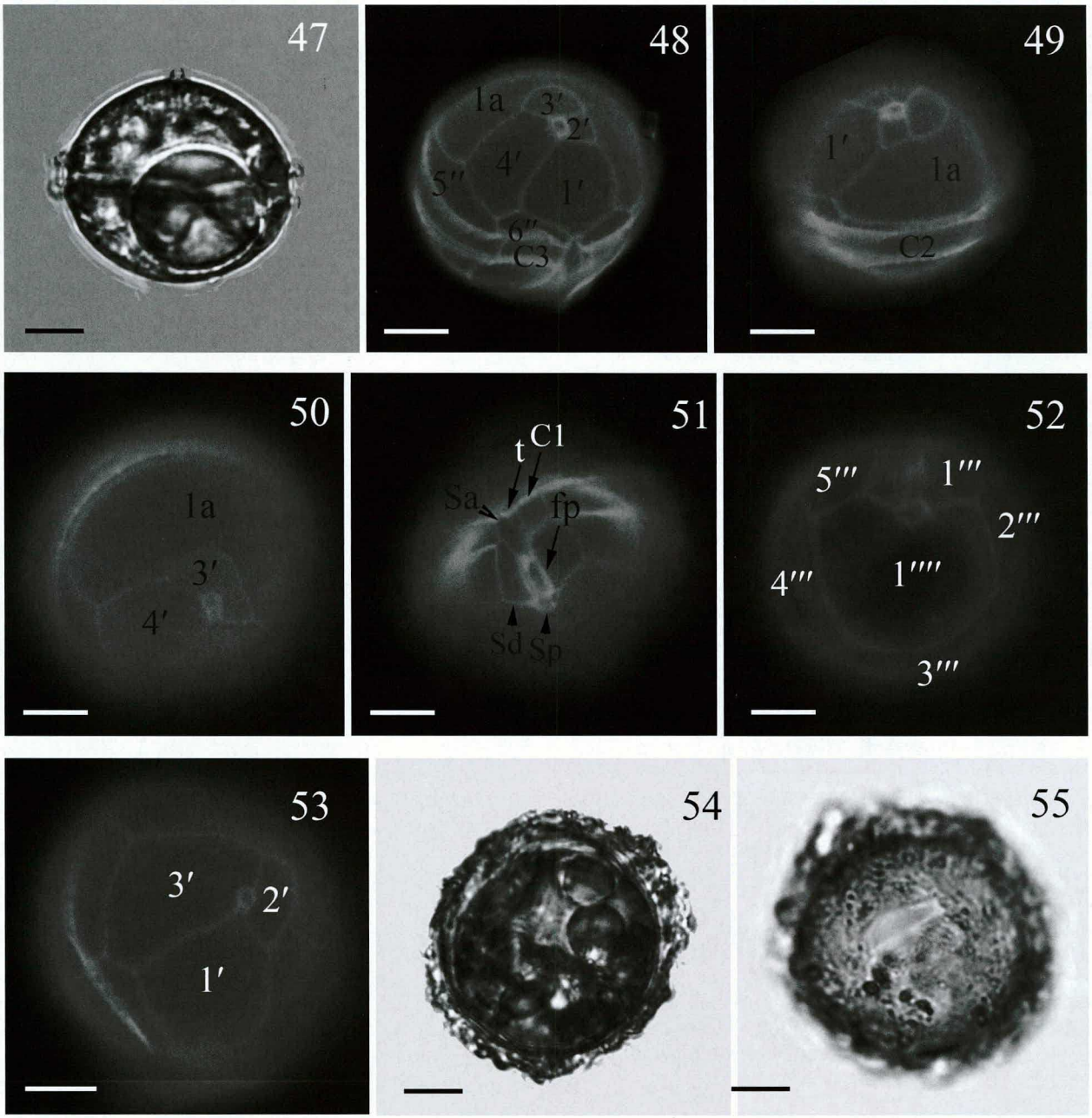

Figs 47–55. LM of vegetative cells and cysts of *B. breve*. Cells in Figs 47–53 were used for sequencing. Scale bars = 10 μm.
Fig. 47. A living cell in ventral view showing the globular shape.
Fig. 48. A calcofluor-stained cell in apical view showing four apical plates.
Figs 49, 50. Calcofluor-stained cells in apical view, showing the anterior intercalary plate.
Fig. 51. A calcofluor-stained cell in ventral view showing the first cingular plates (C1), the transitional plate (t), an anterior sulcal plate (Sa), a right sulcal plate (Sd), a flagellar pore (fp) and a small posterior sulcal plate (Sp).
Fig. 52. A calcofluor-stained cell in antapical view showing five postcingular plates (1‴–5‴) and one antapical plate (1⁗).
Fig. 53. A calcofluor-stained cell in apical view showing three apical plates (1′–3′).
Fig. 54. A living cyst full of granules and covered with mucus.
Fig. 55. An empty cyst showing the theropylic archeopyle.

Preperidinium Mangin
Preperidinium cf. *meunieri*

The motile cells were subglobular with lipid bodies and were pale green. Plate tabulation was Po, X, 3′, 2a, 3C+t, 7″, 3S?, 5‴, 2⁗. The first apical plate (1′) was narrow and ortho-type (Fig. 101). There were two anterior intercalary plates. Plate 2a was heptagonal and large; whereas, plate 1a was much smaller and four-sided (Figs 102, 103). The cingulum was circular and without displacement and had a cingular list with ribs. We were unable to verify the exact number of sulcal plates. The

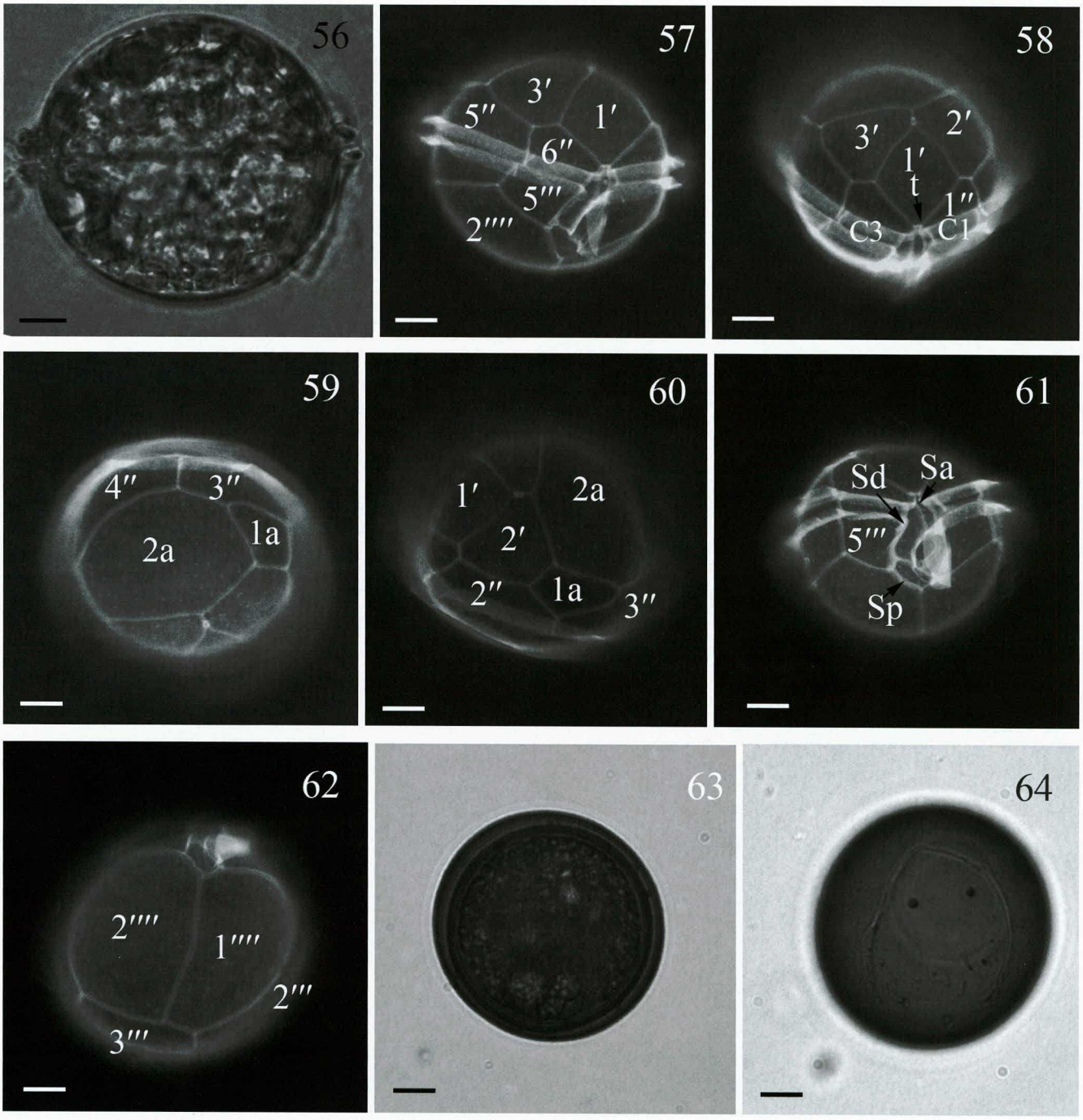

Figs 56–64. LM of vegetative cells and cysts of *D. globula*. Cells in Figs 56–62 were used for sequencing. Scale bars = 10 μm.
Fig. 56. A living cell in ventral view showing the globular shape.
Fig. 57. A calcofluor-stained cell in ventral view, showing the first apical plate (1′) and the prominent sulcal list.
Figs 58–60. Calcofluor-stained cells in apical view, showing three apical plates (1′–3′), two anterior intercalary plates (1a, 2a), two cingular plates (C1, C2), a transitional plate (t) and six precingular plates (1″–6″).
Fig. 61. A calcofluor-stained cell in ventral view, showing an anterior sulcal (Sa) plate, a right sulcal (Sd) plate and a posterior sulcal (Sp) plate.
Fig. 62. A calcofluor-stained cell in antapical view showing five postcingular plates (1‴–5‴) and two antapical plates (1⁗, 2⁗).
Fig. 63. A living cyst full of granules.
Fig. 64. An empty cyst showing the archeopyle.

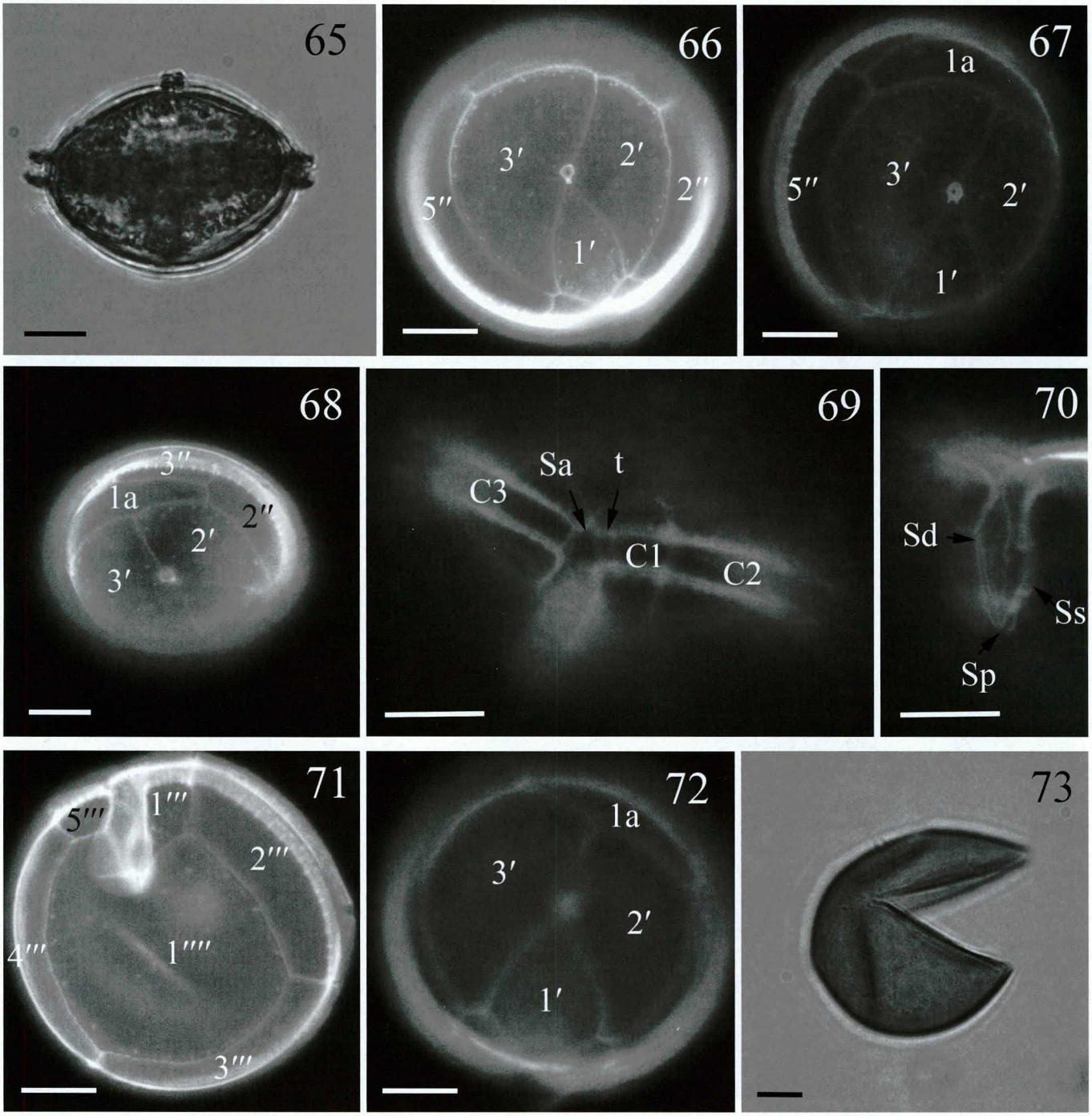

Figs 65–73. LM of vegetative cells and cysts of *D. lenticula*. The cells in Figs 65–71 refer to type A, and the cell in Fig. 72 refers to type B. The cells in Figs 66, 72 were used for sequencing. Scale bars = 10 μm.

Fig. 65. A living cell in ventral view showing the lenticular shape.

Figs 66–68. Calcofluor-stained cells in apical view, showing three apical plates (1′–3′), one anterior intercalary plate (1a) and six precingular plates (1″–6″).

Fig. 69. A calcofluor-stained cell in ventral view, showing an anterior sulcal plate (Sa), three cingular plates and the transitional plate (t).

Fig. 70. A calcofluor-stained cell in ventral view, showing a left sulcal plate (Ss), a right sulcal plate (Sd) and a posterior sulcal plate (Sp).

Fig. 71. Calcofluor-stained cells in antapical view showing five postcingular plates (1‴–5‴) and one antapical plate (1⁗).

Fig. 72. A calcofluor-stained cell in apical view, showing the second and third apical plates (2′, 3′) of equal size.

Fig. 73. An empty cyst showing the archeopyle.

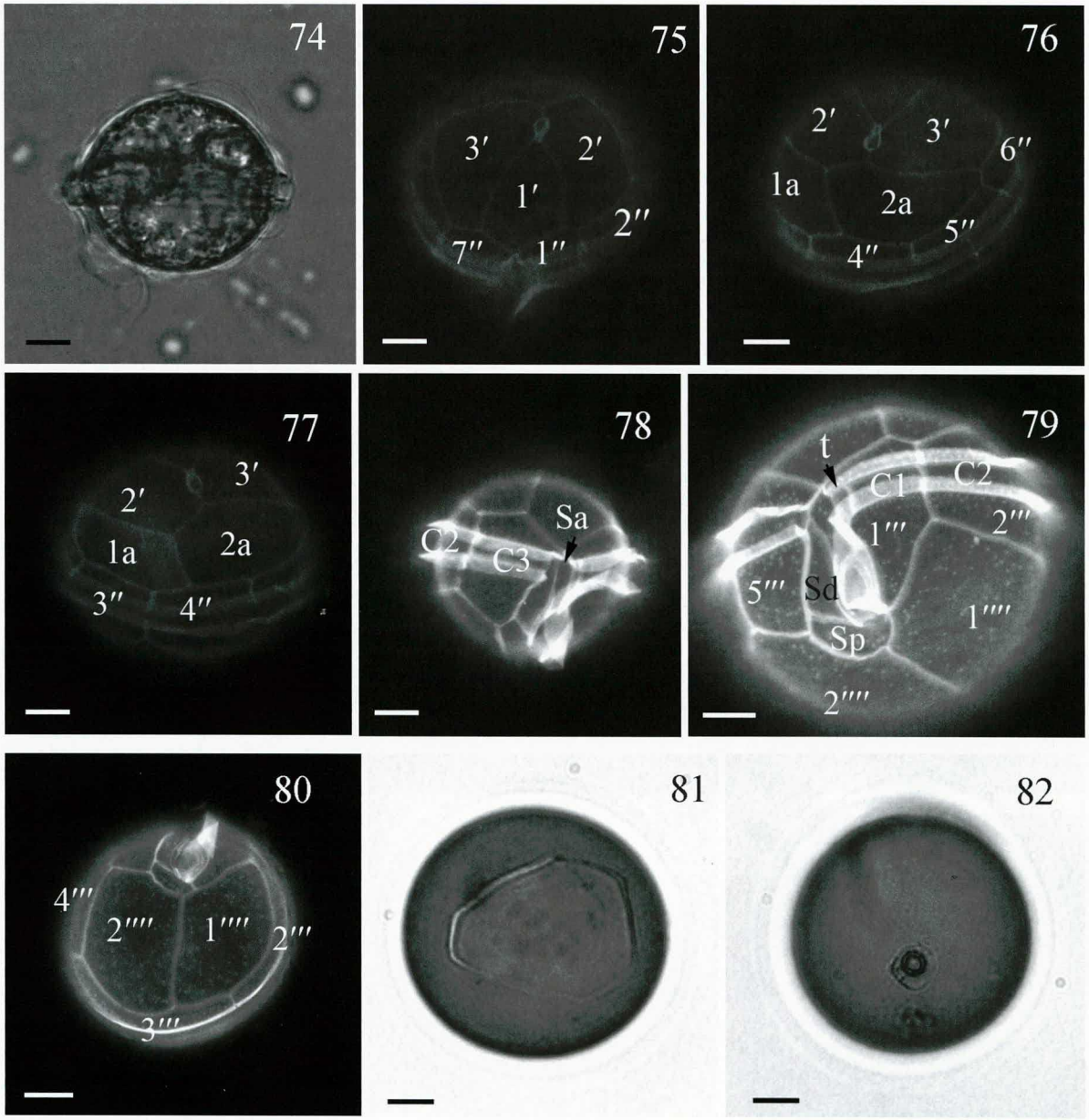

Figs 74–82. LM of vegetative cells and cysts of *D. ovata*. Cells in Figs 74–77 were used for sequencing. Scale bars = 10 μm.

Fig. 74. A living cell in ventral view showing the lenticular shape.

Figs 75–77. Calcofluor-stained cells in apical view, showing three apical plates, two anterior intercalary plates (1a, 2a) and seven precingular plates (1″–7″).

Fig. 78. A calcofluor-stained cell in ventral view, showing the second and third cingular plates (C2, C3).

Fig. 79. A calcofluor-stained cell in ventral view, showing the first cingular plate (C1), the transitional plate (t), the prominent sulcal list, a right sulcal plate (Sd) and a posterior sulcal plate (Sp).

Fig. 80. A calcofluor-stained cell in antapical view showing five postcingular plates (1‴–5‴) and two antapical plates (1⁗, 2⁗).

Fig. 81. An empty cyst showing the archeopyle.

Fig. 82. An empty cyst showing the flagellar scar.

cells had an A type of the Sa plate *sensu* Dodge & Hermes (1981) (Figs 101, 104). The Sp plate was very small and of the Caspica-type (Fig. 105). There were five four-sided postcingular plates and one large antapical plate (Figs 104, 105). Cysts were dark brown, round in apical view and full of granules (Fig. 106).

The incubated motile cell was 46.2 μm in length and 50.0 μm in width ($n = 1$). The cyst germinated to give an identifiable theca 50.0 μm in width and 46.6 μm in length ($n = 1$).

Based on both theca morphology and molecular phylogeny, a hypothetical evolution of the subfamily Diplopsalioideae is presented in Figs 107, 108.

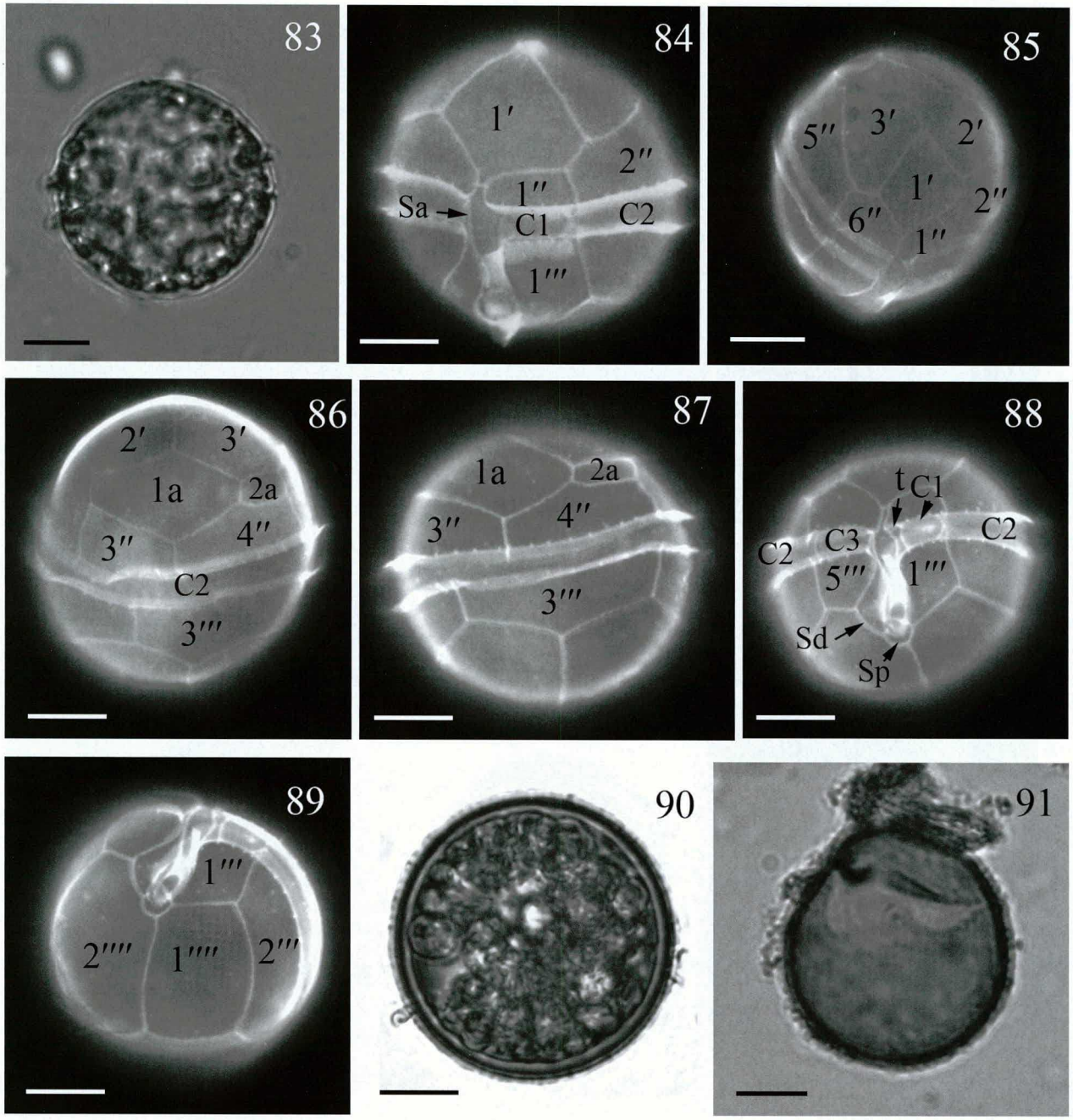

Figs 83–91. LM of vegetative cells and cysts of *L. pusilla*. The cell in Figs 84, 87 was used for sequencing. Scale bars = 10 μm.

Fig. 83. A living cell in ventral view showing the globular shape.

Fig. 84. A calcofluor-stained cell in ventral view, showing the meta first apical plate (1′).

Fig. 85. A calcofluor-stained cell in apical view, showing the second and third apical plates (2′, 3′).

Figs 86, 87. Calcofluor-stained cells in dorsal view, showing two anterior intercalary plates (1a, 2a).

Fig. 88. A calcofluor-stained cell in ventral view, showing three cingular plates (C1–C3), the transitional plate (t), a prominent sulcal list, a right sulcal (Sd) plate and a posterior sulcal (Sp) plate.

Fig. 89. A calcofluor-stained cell in antapical view showing five postcingular plates (1‴–5‴) and two antapical plates (1⁗, 2⁗).

Fig. 90. A living cyst full of granules.

Fig. 91. An empty cyst showing the archeopyle.

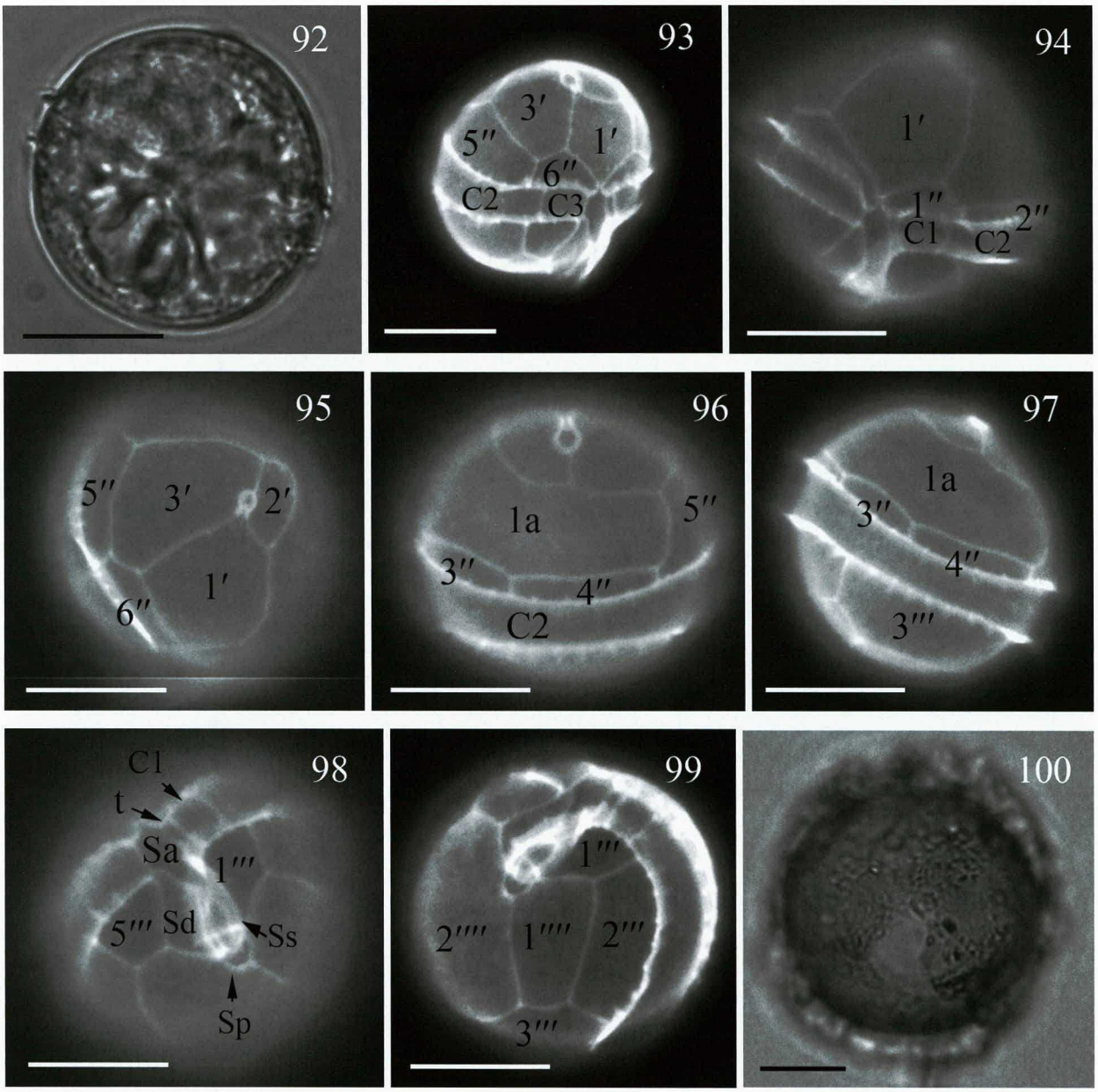

Figs 92–100. LM of vegetative cells and cysts of *O. rotunda*. Cell in Fig. 94 was used for sequencing. Scale bars = 10 μm.
Fig. 92. A living cell in ventral view showing the globular shape.
Fig. 93. A calcofluor-stained cell in right lateral view showing the second and third cingular plate (C2, C3).
Fig. 94. A calcofluor-stained cell in ventral view, showing the meta 1′ and the first cingular plate (C1).
Fig. 95. A calcofluor-stained cell in apical view, showing three apical plates (1′–3′).
Figs 96, 97. Calcofluor-stained cells in dorsal view, showing the large anterior intercalary (1a) plate and second cingular plate (C2).
Fig. 98. A calcofluor-stained cell in ventral view showing the first cingular plate (C1), the transitional plate (t), a prominent sulcal list, an anterior sulcal plate (Sa), a right sulcal plate (Sd), a left sulcal plate (Ss) and a small posterior sulcal plate (Sp).
Fig. 99. A calcofluor-stained cell in antapical view showing five postcingular plates (1‴–5‴) and two antapical plates (1⁗, 2⁗).
Fig. 100. An empty cyst showing the theropylic intercalary archeopyle.

DISCUSSION

Morphological considerations

We chose to maintain the status quo as much as possible and considered one plate difference in the epithecal or hypothecal series sufficient to warrant placement in a different genus. This was largely consistent with the molecular phylogenetics, where every genus formed a monophyletic clade (Fig. 1). The only genus that raised some issues was *Qia*, which has a separate clade in the phylogeny (Fig. 1) but a quasi-identical plate formula as the genus *Diplopsalis*. Below we discuss the found species and compare them to closely related species.

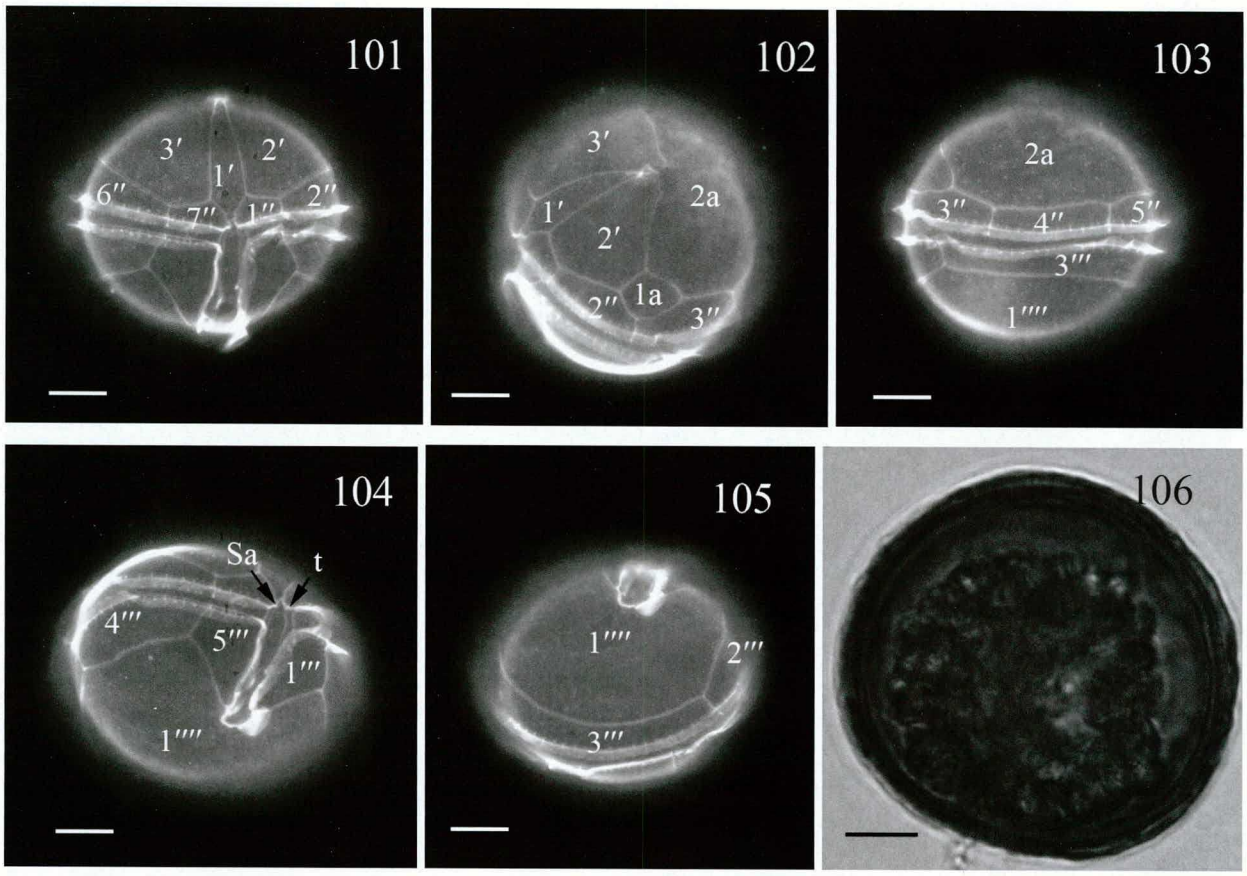

Figs 101–106. LM of vegetative cells and cysts of *Preperidinium* cf. *meunieri*. Cell in Figs 101–105 was used for sequencing. Scale bars = 10 μm.
Fig. 101. A calcofluor-stained cell in ventral view showing the subglobular shape and an ortho-type first apical plate (1′).
Fig. 102. A calcofluor-stained cell in left lateral view showing two anterior intercalary plates (1a, 2a).
Fig. 103. A calcofluor-stained cell in dorsal view showing the second anterior intercalary plates (2a).
Fig. 104. A calcofluor-stained cell in ventral-antapical view showing the transitional plate (t) and an anterior sulcal (Sa) plate.
Fig. 105. A calcofluor-stained cell in antapical view showing one large antapical plate (1⁗).
Fig. 106. A living cyst full of granules.

The genus *Niea* can be differentiated from *Diplopsalis* because it has two antapical plates and from *Oblea* because it has an ortho first apical plate (1′). The theca of Chinese *N. acanthocysta* fits the original description (Kawami *et al.* 2006, as *O. acanthocysta*), and the cyst conforms to the revised description (Mertens *et al.* 2015). Our specimens of *N. torta* are characterized by a large cell size and a markedly inclined 1a plate and are thus morphologically similar to those described by Abé (1941, as *O. torta*) and Nie (1943, as *D. hainanensis*). *Niea chinensis* has the same plate formula as *N. acanthocysta*, but *N. chinensis* has globular cells; whereas, *N. acanthocysta* is somewhat lenticular. *Niea chinensis* also differs from *N. acanthocysta* in the configuration of the 1a plate, which is located in the middle of the dorsal epitheca in *N. chinensis* compared to slight inclination to the left in *N. acanthocysta* (Kawami *et al.* 2006). *Niea chinensis* differs from *N. torta* in the small cell size and a symmetrical epitheca (Abé 1941). Cysts of these three species are also quite different. *Niea acanthocysta* has a spiny cyst; whereas, those of *N. chinensis* and *N. torta* are smooth. *Niea chinensis* differs from *N. torta* in having an intercalary archeopyle in contrast to a theropylic epicystal archeopyle of *N. torta*.

Chinese cells of *D. lenticula* type A have an asymmetrical 2′ and 3′ and are morphologically similar to those reported from the South China Sea (Nie 1943) and Japanese waters (Matsuoka 1988). Chinese cells of *D. lenticula* type B have a symmetrical 2′ and 3′, thus conforming to the type specimen (Bergh & Daday 1881) and other specimens reported from Europe (Schiller 1937; Dodge & Hermes 1981). Both cell types of *D. lenticula* were recovered from the Gulf of Mexico (Gribble & Anderson 2006), and their cyst morphologies are stable (Matsuoka 1988; Lewis 1990; Ellegaard *et al.* 1994; present study), suggesting that configuration of 2′ and 3′ might be plastic in *D. lenticula*.

Diplopsalis lebouriae was originally regarded as a variety of *D. lenticula* (Nie 1943); however, we transfer it to a new genus, *Qia*, based on the shape of the anterior intercalary plate and the molecular phylogeny. Chinese cells of *Q. lebouriae* from both types of cysts are morphologically similar, and they share an A type of Sa plate *sensu* Dodge & Hermes (1981), unlike the type species described from Hainan (China), which has a C type *sensu* Dodge & Hermes (1981; Nie 1943, fig. 14). Because Sa is so small, we suggest that it might have been overlooked by Nie (1943). Smooth cysts of *Q. lebouriae* have been reported before (Wall & Dale 1968, pl. 4, fig. 19, text fig. 7,

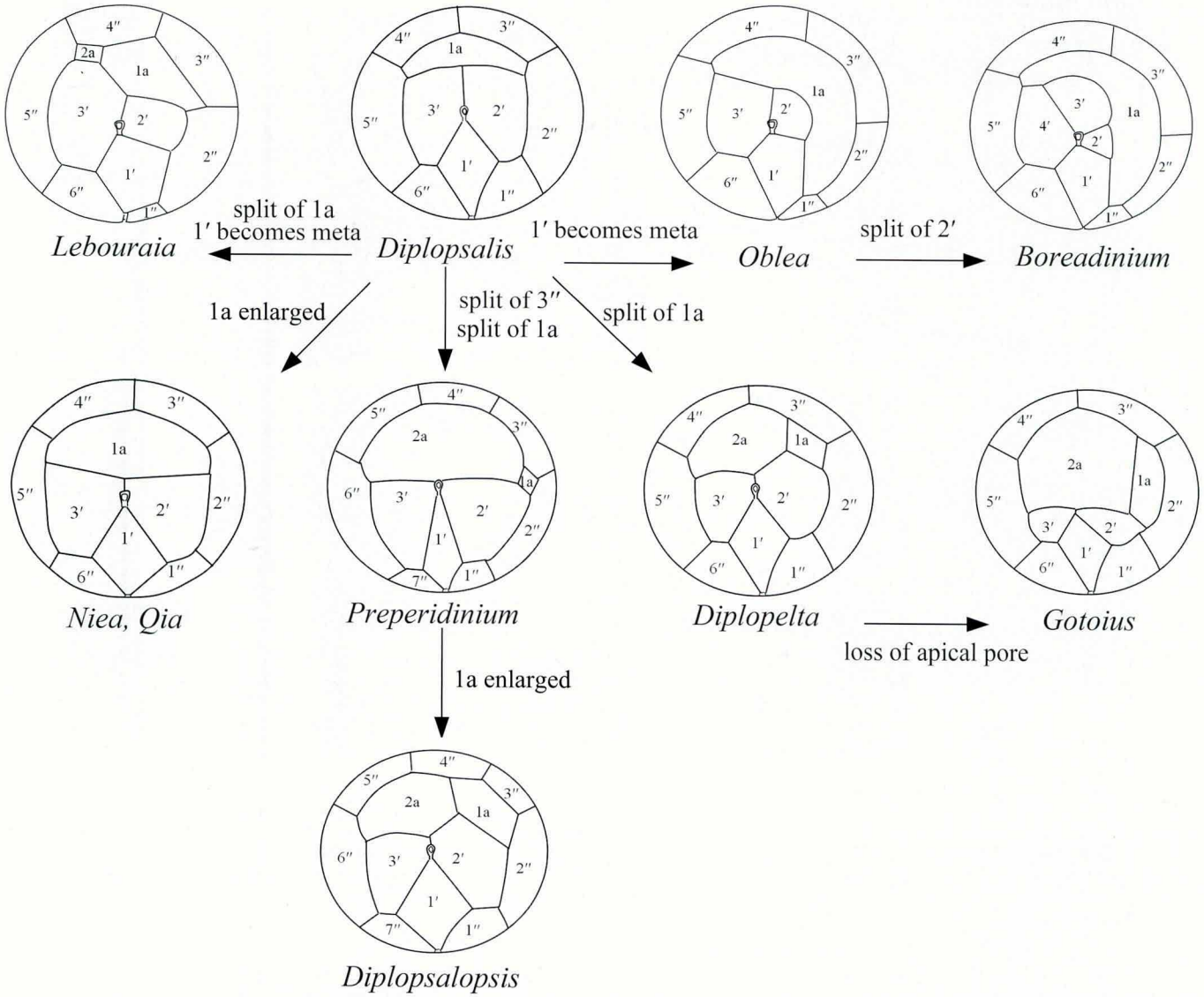

Fig. 107. A hypothetical evolution on the epitheca of the diplopsalioideans.

misidentified as *D. lenticula*; see Matsuoka 1988, p. 103) as well as specimens with granular cyst walls (Matsuoka 1988, as *D. lebouriae*), and here we provide evidence that it can also produce spiny cysts. Various cyst types of *Q. lebouriae* might represent different species because cyst morphology has been regarded as a key feature to separate different genera of diplopsalioideans (Matsuoka 1988).

The motile stages of Chinese *D. globula* differ from specimens from Shimoda Bay, Japan, in possessing a smaller apical pore and a circular cingulum without displacement in the former (Abé 1941). Our cells of *Diplops. ovata* fit the original description (Abé 1941, as *Diplopsalopsis orbicularis* var. *ovata* Abé). *Diplopsalopsis ovata* differs from *Diplops. orbicularis* by possessing a much larger plate 1a. Moreover, the Sa plate of *Diplops. ovata* is type A; whereas, that of *Diplops. orbicularis* is type C (Dodge & Hermes 1981).

The motile stage of *L. pusilla* is similar to specimens described by Balech and Akselman (1988), except that the 2a plate of our cells is narrower. A similar cyst was reported from Australia and was identified as corresponding to *Lebouraia minuta* T. H. Abé (Sonneman & Hill 1997), but its first apical plate was wide and contacted the Sa plate, suggesting that it might be *L. pusilla* instead.

Both theca and cyst morphology of Chinese *O. rotunda* are identical to those reported by Lewis (1990). Our cells of *B. breve* fit the original description (Abé 1981) and differ from *B. pisiforme* Dodge & Hermes in having six instead of seven precingular plates (Dodge & Hermes 1981). *Boreadinium* differs from *Oblea* in having four apical plates instead of three and one antapical plate instead of two and in the shape of Sa plate (B-type vs C-type). *Preperidinium* cf. *meunieri* is morphologically similar to the type species but differs in having a more globular cell shape (Paulsen 1908).

Molecular phylogeny and morphological evolution

The 22 new LSU rDNA sequences obtained in the present study allow us to speculate on the morphological evolution of

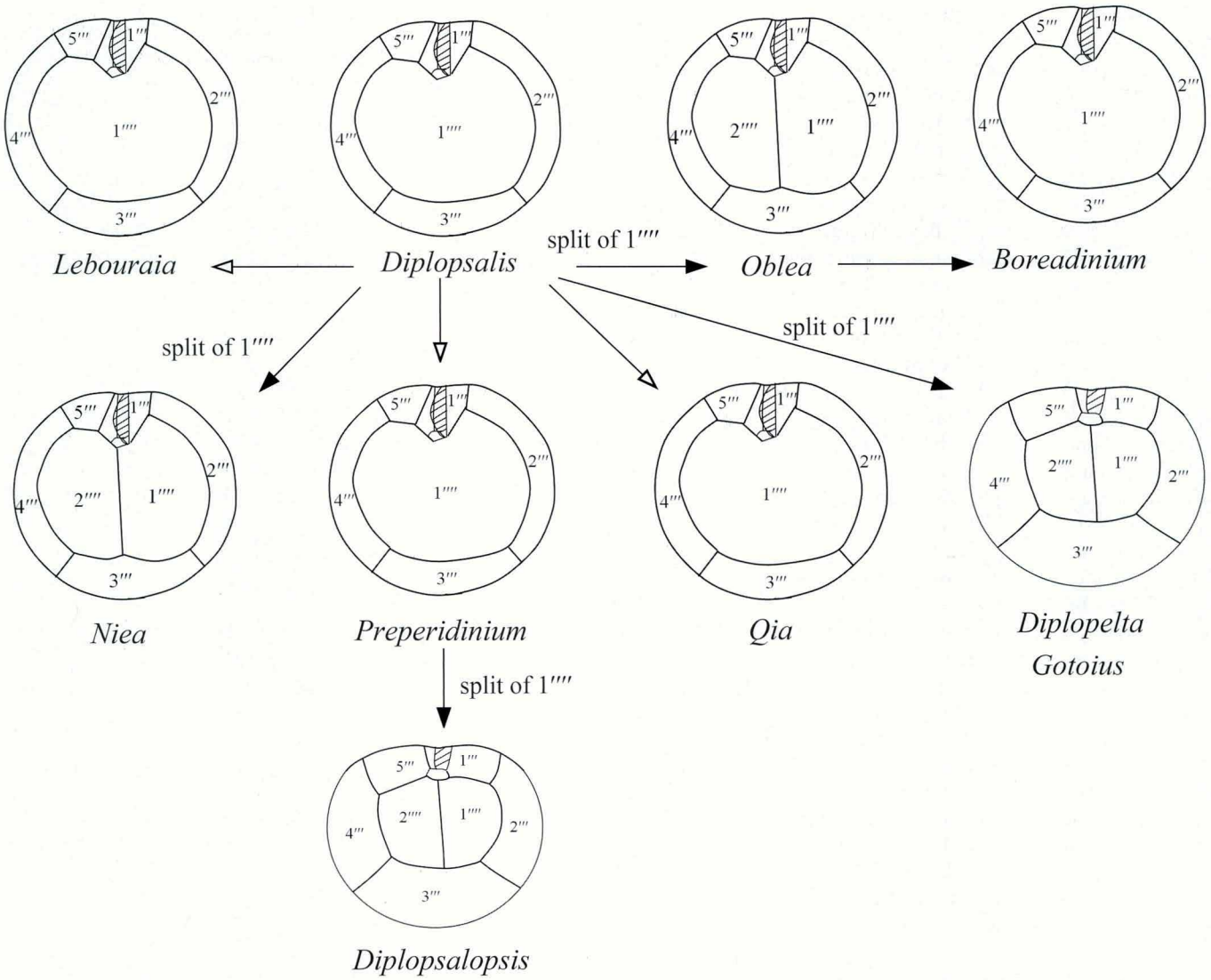

Fig. 108. A hypothetical evolution on the hypotheca of the diplopsalioideans. White arrowheads indicate that there was no variation in the tabulation of the hypotheca.

the diplopsalioideans (Figs 107, 108). Our updated molecular phylogeny support the evolution of *Diplopsalopsis* from *Diplopsalis via Preperidinium* as proposed by Lebour (1922), suggesting that plate increase occurred during evolution of the diplopsalioideans. Our results also demonstrate that the epitheca evolved faster than the hypotheca in the diplopsalioideans (Figs 107, 108); this supports the notion that the hypotheca is much more conservative in dinoflagellates (Balech 1980).

Several morphological characteristics are homoplasious in the molecular phylogeny, and our results do not support the two groups (subgroup I and subgroup II) of the diplopsalioideans based on the number of antapical plates (Dodge & Hermes 1981). This has been regarded as a conservative character (Balech 1980). The type of the Sa plate is polyphyletic because type A is present throughout the three clades, and type C was reported in *Boreadinium* and *D. orbicularis* (Paulsen) Meunier (Abé 1941; Dodge & Hermes 1981).

Other morphological characters are synapomorphies in the molecular phylogeny, and our results support the systematic importance of the posterior sulcal (Sp) plate (Abé 1981). The Caspica-type of the Sp plate is present throughout the three clades, but the Asymmetrica-type was found only in *D. globula* and *Diplops. ovata* in clade III, suggesting that the latter might be a derived feature.

The specific plate formulas – and thus most generic descriptions of the diplopsalioideans – are monophyletic in the molecular phylogeny (Fig. 1, Table 2). However, several genera with identical plate formulas can be differentiated by the shape of plate 1a or 1′. This suggests that these two morphological characteristics are especially important at the intergeneric level. The genus *Qia* differs from *Diplopsalis* only in the shape of the 1a plate, and their separation was supported by the molecular phylogeny based on LSU rDNA (Mertens *et al.* 2015; present study) as well as on SSU rDNA (Mertens *et al.* 2015). *Qia lebouriae* has a hexagonal 1a plate close to the apical pore; whereas, *D. lenticula* (the type species

of *Diplopsalis*) has a rectangular 1a plate in the low part of the epitheca. *Diplopsalis caspica* Ostenfeld has a small diamond-shaped 1a plate (Ostenfeld 1901) whose closest relative cannot be identified and thus probably belongs to another new genus.

The genus *Niea* differs from *Oblea* only in the shape of plates 1′ and 1a. The presence of a meta 1′ was reported in *Oblea*, *Boreadinium* and *Lebouraia* (Dodge & Toriumi 1993; present study). These genera were classified in clade I (Fig. 1), suggesting that they might have diverged earlier. *Oblea* and *Boreadinium* have a very large 1a plate; whereas, *Lebouraia* has a large 1a plate together with a small 2a plate. This configuration of the anterior intercalary plates was not observed in other genera of the diplopsalioideans. The number of anterior intercalary plates and the shape of 1′ were used only to subdivide *Protoperidinium* at subgeneric and sectional ranks (Balech 1974; Taylor 1976), suggesting that rapid diversification occurred in the diplopsalioideans.

It is also important to note that the genera *Diplopelta* and *Gotoius* share an identical plate pattern, except that *Diplopelta* has an apical pore and *Gotoius* does not have one. The presence or absence of such an apical pore was regarded as a subgeneric feature of *Protoperidinium* (Faust 2006) and *Peridinium* (Balech 1988), and therefore *Gotoius* might be a junior synonym of *Diplopelta*. Furthermore, whether both of the species assigned to *Boreadinium* belong to this genus is questionable since *B. breve* has six precingular plates instead of the seven in *B. pisiforme* J.D. Dodge & H.B. Hermes. This can be clarified only when a sequence of *B. pisiforme* (the type species of *Boreadinium*) becomes available. Although our molecular phylogeny covers almost all genera of the diplopsalioideans, sequences from the type species of many genera (e.g. *Gotoius mutsuensis* T.H. Abé ex Matsuoka, *O. baculifera* Balech *ex* Loeblich & A.R. Loeblich, *L. minuta*, *D. orbicularis*) are still not available and will be the focus of future work.

ACKNOWLEDGEMENTS

This project was supported by National Natural Science Foundation of China (41376170). K.N.M. is a postdoctoral fellow of FWO Belgium. Two anonymous reviewers and the editor are thanked for constructive comments that significantly improved the article.

SUPPLEMENTARY DATA

Supplementary data associated with this article can be found online at http://dx.doi.org/10.2216/14–94.1.s1.

REFERENCES

Abé T. 1941. Studies on protozoan fauna of Shimoda Bay. The *Diplopsalis* group. *Records of Oceanographic Works in Japan* 12: 121–144.

Abé T. 1981. Studies on the family Peridiniales. *Seto Marine Biological Laboratory, Special Publication Series* 6:1–409.

Balech E. 1964. El plancton de Mar del Plata durante el periodo 1961–1962. *Instituto de Biologia Marina* 4: 1–49.

Balech E. 1974. El Genero '*Protoperidinium*' Bergh, 1881 (*Peridinium* Ehrenberg, 1831, partim). *Revista del Museo Argentino de Ciencias Naturales 'Bernardino Rivadavia' e Instituto Nacional de Investigación de las Ciencias Naturales* 4: 1–79.

Balech E. 1980. On the thecal morphology of dinoflagellates with special emphasis on circular and sulcal plates. *Anales del Centro de Ciencias del Mar y Limnologia, Universidad Nacional Autonomia de Mexico* 7: 57–68.

Balech E. 1988. Los dinoflagellados del Atlantico sudoccidental. *Publicaciones Especiales Instituto Español de Oceanografia* 1: 1–310.

Balech E. & Akselman R. 1988. Un nuevo Diplopsaliinae (Dinoflagellatae) de Patagonia, Argentina. *Physis (Buenos Aires)* A46: 27–30.

Bergh R.S. & Daday J. 1881. Der organismus der cilioflagellaten: eine phylogenetische studie. *Morphologisches Jahrbuch* 7: 12–128.

Boc A., Diallo A.B. & Makarenkov V. 2012. T-REX: a web server for inferring, validating and visualizing phylogenetic trees and networks. *Nucleic Acids Research* 40: W573–W579.

Chomérat N., Couté A., Fayolle S., Mascarell G. & Cazaubon A. 2004. Morphology and ecology of *Oblea rotunda* (Diplopsalidaceae, Dinophyceae) from a new habitat: a brackish and hypertrophic ecosystem, the Étang de Bolmon (South of France). *European Journal of Phycology* 39: 317–326.

Dale B., Montresor M., Zingone A. & Zonneveld K. 1993. The cyst-motile stage relationships of the dinoflagellates *Diplopelta symmetrica* and *Diplopsalopsis latipeltata*. *European Journal of Phycology* 28: 129–137.

Daugbjerg N., Hansen G., Larsen J. & Moestrup Ø. 2000. Phylogeny of some of the major genera of dinoflagellates based on ultrastructure and partial LSU rDNA sequence data, including the erection of three new genera of unarmoured dinoflagellates. *Phycologia* 39: 302–317.

Dodge J.D. & Hermes H. 1981. A revision of the *Diplopsalis* group of dinoflagellates based on marterial from the British Isles. *Botanical Journal of the Linnean Society* 83: 15–26.

Dodge J.D. & Toriumi S. 1993. A taxonomic revision of the *Diplopsalis* group (Dinophyceae). *Botanica Marina* 36: 137–147.

Elbrächter M. 1993. *Kolkwitziella* Lindemann 1919 and *Preperidinium* Mangin 1913: correct genera names in the *Diplopsalis*-group (Dinophyceae). *Nova Hedwigia* 56: 173–178.

Ellegaard M., Christensen N.F. & Moestrup Ø. 1994. Dinoflagellate cysts from recent Danish marine sediments. *European Journal of Phycology* 29: 183–194.

Faust M.A. 2006. Creation of the subgenus *Testeria* Faust *subgen. nov.* *Protoperidinium* Bergh from the SW Atlantic Ocean: *Protoperidinium novella* sp. nov. and *Protoperidinium concinna* sp. nov. Dinophyceae. *Phycologia* 45: 1–9.

Fensome R.A., Taylor F.J.R., Norris G., Sarjeant W.A.S., Wharton D.I. & Williams G.L. 1993. A classification of fossil and living dinoflagellates. *Micropaleontology Special Publication* 7: 1–245.

Fritz L. & Triemer R. 1985. A rapid simple technique utilizing calcofluor white M2R for the visualization of dinoflagellate thecal plates. *Journal of Phycology* 21: 662–664.

Gribble K.E. & Anderson D.M. 2006. Molecular phylogeny of the heterotrophic dinoflagellates, *Protoperidinium*, *Diplopsalis* and *Preperidinium* (Dinophyceae), inferred from large subunit rDNA. *Journal of Phycology* 42: 1081–1095.

Gu H., Liu T., & Mertens K.N. 2015. Cyst-theca relationship and phylogenetic positions of *Protoperidinium* (Peridiniales, Dinophyceae) species of the sections *Conica* and *Tabulata*, with description of *Protoperidinium shanghaiense* sp. nov. *Phycologia* DOI:10.2216/14–047.1.

Guillard R.R.L. & Ryther J.H. 1962. Studies of marine planktonic diatoms. I. *Cyclotella nana* Hustedt and *Detonula confervacea* Cleve. *Canadian Journal of Microbiology* 8: 229–239.

Hall T.A. 1999. BioEdit: a user-friendly biological sequence alignment editor and analysis program for Windows 95/98/NT. *Nucleic Acids Symposium Series* 41: 95–98.

Harland R. 1982. A review of recent and quaternary organic-walled dinoflagellate cysts of the genus *Protoperidinium*. *Palaeontology* 25: 369–397.

KATOH K., KUMA K., TOH H. & MIYATA T. 2005. MAFFT version 5: improvement in accuracy of multiple sequence alignment. *Nucleic Acids Research* 33: 511–518.

KAWAMI H., IWATAKI M. & MATSUOKA K. 2006. A new diplopsalid species *Oblea acanthocysta* sp. nov. (Peridiniales, Dinophyceae). *Plankton and Benthos Research* 1: 183–190.

LEBOUR M.V. 1922. Plymouth peridinians: I. *Diplopsalis lenticula* and its relatives. *Journal of the Marine Biological Association of the United Kingdom* 12: 795–812.

LEWIS J. 1990. The cyst-theca relationship of *Oblea rotunda* (Diplopsalidaceae, Dinophyceae). *British Phycological Journal* 25: 339–351.

LIU T., GU H., MERTENS K. & LAN D. 2014. New dinoflagellate species *Protoperidinium haizhouense* sp. nov. (Peridiniales, Dinophyceae), its cyst-theca relationship and phylogenetic position within the Monovela group. *Phycological Research* 62: 109–124.

LIU T., MERTENS K.N., RIBEIRO S., ELLEGAARD M., MATSUOKA H. & GU H. 2015. Cyst-theca relationships and phylogenetic positions of Peridiniales (Dinophyceae) with two anterior intercalary plates, with description of *Archaeperidinium bailongense* sp. nov. and *Protoperidinium fuzhouense* sp. nov. *Phycological Research* DOI:10.1111/pre.12081.

MATSUOKA K. 1988. Cyst-theca relationships in the diplopsalid group (Peridiniales, Dinophyceae). *Review of Palaeobotany and Palynology* 56: 95–122.

MATSUOKA K. & KAWAMI H. 2013. Phylogenetic subdivision of the genus *Protoperidinium*, (Peridiniales, Dinophyceae) with emphasis on the Monovela Group. In: *Biological and geological perspectives of dinoflagellates* (Ed. by J.M. Lewis, F. Marret & L. Bradley), pp.267–276. The Micropalaeontological Society, Special Publications. Geological Society, London.

MERTENS K.N., TAKANO Y., GU H., YAMAGUCHI A., POSPELOVA V., ELLEGAARD M. & MATSUOKA K. 2015. The cyst-theca relationship of a new dinoflagellate with a spiny round brown cyst, *Protoperidinium lewisiae*, and its comparison to the cyst of *Oblea acanthocysta*. *Phycological Research* DOI:10.1111/pre.12083.

NIE D. 1943. Dinoflagellata of the Hainan region VI. on the genus *Diplopsalis*. *Sinensia* 14: 1–21.

OSTENFELD C.H. 1901. Phytoplankton fra det Kaspiske Hav. *Videnskabelige Meddelelser fra den naturhistoriske Forening i Kjøbenhavn* 1901: 129–139.

PAULSEN O. 1908. Peridiniales. Nordisches Plankton. Botanischer Teil 18: 1–124.

PAVILLARD J. 1913. *Le genre Diplopsalis Bergh et les genres voisins. Montpellier*, pp. 1–12.

POSADA D. 2008. jModelTest: phylogenetic model averaging. *Molecular Biology and Evolution* 25: 1253–1256.

RONQUIST F. & HUELSENBECK J.P. 2003. MrBayes 3: Bayesian phylogenetic inference under mixed models. *Bioinformatics* 19: 1572–1574.

SCHILLER J. 1937. Dinoflagellatae (Peridineae) in monographischer Behandlung. In: *Kryptogamen-Flora von Deutschland, Österreich und der Schweiz* (Ed. by L. Rabenhorst), pp. 1–589. Akademische, Leipzig.

SCHOLIN C.A., HERZOG M., SOGIN M. & ANDERSON D.M. 1994. Identification of group- and strain-specific genetic markers for globally distributed *Alexandrium* (Dinophyceae). II. Sequence analysis of a fragment of the LSU rRNA gene. *Journal of Phycology* 30: 999–1011.

SONNEMAN J. & HILL D. 1997. A taxonomic survey of cyst-producing dinoflagellates from recent sediments of Victorian coastal waters, Australia. *Botanica Marina* 40: 149–178.

SOURNIA A. 1973. La production primaire planctonique en Méditerranée. Essai de mise à jour, *Bulletin de l'Étude en commun de la Méditerranée, numéro spécial* 5: 1–128.

STAMATAKIS A. 2006. RAxML-VI-HPC: maximum likelihood-based phylogenetic analyses with thousands of taxa and mixed models. *Bioinformatics* 22: 2688–2690.

TAYLOR F. 1976. Dinoflagellates from the International Indian Ocean Expedition. *Biblotheca Botanica* 132: 1–234.

WALL D. & DALE B. 1968. Modern dinoflagellate cysts and evolution of the Peridiniales. *Micropaleontology* 14: 265–304.

Received 22 October 2014; accepted 3 February 2015